Flexibility From Distributed Multienergy Systems

INVITED PAPER

Flexibility From Distributed Multienergy Systems

By Gianfranco Chicco, *Fellow IEEE*, Shariq Riaz, *Member IEEE*, Andrea Mazza, *Member IEEE*, and Pierluigi Mancarella, *Senior Member IEEE*

ABSTRACT | Multienergy systems (MES), in which multiple energy vectors are integrated and optimally operated, are key assets in low-carbon energy systems. Multienergy interactions of distributed energy resources via different energy networks generate the so-called distributed MES (DMES). While it is now well recognized that DMES can provide power system flexibility by shifting across different energy vectors, it is essential to have a systematic discussion on the main features of such flexibility. This article presents a comprehensive overview of DMES modeling and characterization of flexibility applications. The concept of "multienergy node" is introduced to extend the power node model, used for electrical flexibility, in the multienergy case. A general definition of DMES flexibility is given, and a general mathematical and graphical modeling framework, based on multidimensional maps, is formulated to describe the operational characteristics of individual MES and aggregate DMES, including the role of multienergy networks in enabling or constraining flexibility. Several tutorial examples are finally presented with illustrative case studies on current and future DMES practical applications.

KEYWORDS | Energy hub; energy systems integration; flexibility; grid services; hydrogen; multienergy arbitrage; multienergy node; multienergy system; power node; power-to-gas; power-to-heat; virtual battery.

Manuscript received November 18, 2019; revised March 4, 2020; accepted April 3, 2020. The work of Shariq Riaz was supported in part by Veski and the Victorian Government, Australia, through the FlexCity Project. The work of Pierluigi Mancarella was supported in part by Veski and the Victorian Government, Australia, through the FlexCity Project, and in part by the U.K. Engineering and Physical Sciences Research Council (EPSRC) through the MY-STORE Project under Grant EP/N001974/1. *(Corresponding author: Gianfranco Chicco.)*

Gianfranco Chicco and **Andrea Mazza** are with the Dipartimento Energia "Galileo Ferraris," Politecnico di Torino, 10129 Turin, Italy (e-mail: gianfranco.chicco@polito.it; andrea.mazza@polito.it).

Shariq Riaz is with the Department of Electrical and Electronic Engineering, The University of Melbourne, Melbourne, VIC 3010, Australia (e-mail: shariq.riaz@unimelb.edu.au).

Pierluigi Mancarella is with the Department of Electrical and Electronic Engineering, The University of Melbourne, Melbourne, VIC 3010, Australia, and also with the Department of Electrical and Electronic Engineering, The University of Manchester, Manchester M13 9PL, U.K. (e-mail: pierluigi.mancarella@unimelb.edu.au).

Digital Object Identifier 10.1109/JPROC.2020.2986378

I. INTRODUCTION

A. General Context

The historical transition toward low-carbon power and energy systems is primarily based on the integration of renewable energy sources (RESs), low-carbon technologies (LCTs), and distributed energy resources (DERs), and is bringing unprecedented challenges to system operation. Among others, there are major flexibility challenges that are linked to operating a system with large shares of variable and partly unpredictable RES and DER [1], [2]. There have always been requirements for flexibility in power systems, for example, to deal with balancing demand and peak times. However, the supply–demand operational variability and uncertainty affecting both current and future systems are much greater [3], [4] and the traditional providers of flexibility, e.g., conventional power plants such as combined cycle and open-cycle gas turbines, diesel generators, and so on, are being displaced due to commercial or environmental reasons. New means to provide flexibility are therefore needed, while some of the flexible LCT, for example, batteries, may still be relatively expensive or inadequate, depending on the specific requirements.

In the same context of energy decarbonization, multienergy systems (MES) [5], in which multiple energy vectors (such as electric heat, cooling, gas, hydrogen, etc.) are optimally integrated and operated, are now generally recognized to be key to delivering affordable and reliable low-carbon energy systems, particularly in the light of increasing whole-system energy efficiency and enabling whole-system decarbonization [6]. In addition to the general interest in MES to decarbonize the whole energy sector (beyond electricity) at a lower cost via energy systems integration, further benefits are arising from multienergy

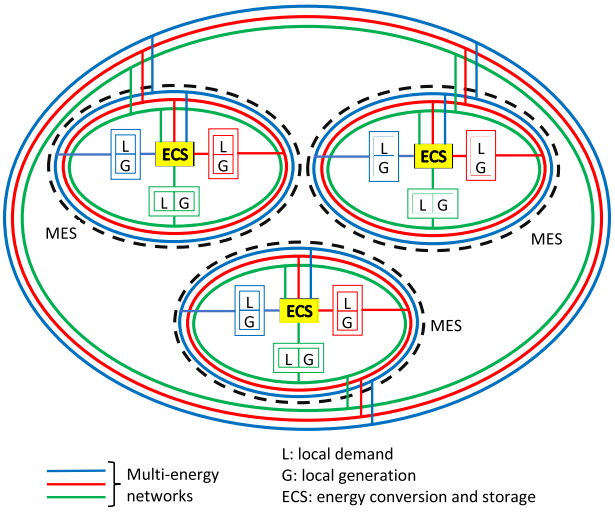

Fig. 1. ***Schematic of DMES as an aggregation of multiple MES, illustrating the scalability of the concept at multiple aggregation levels.***

vector system operation. In this respect, MES exhibit an exceptional potential to unlock value somehow hidden when considering only electricity, and access new forms of flexibility, particularly on the demand side, which, as aforementioned, may be essential in RES-based energy systems [7]. In particular, as several major multienergy interactions take place through DER and involve multiple energy networks, there is a great interest in and potential flexibility options arising from distributed MES (DMES). A DMES is defined as composed of multiple local MES plants interconnected through multienergy networks (see Fig. 1). Modeling a DMES requires an active view of the different plant components introduced earlier, their connections, and the energy conversions and conditioning that occur inside the system. The DMES concept is completely scalable, as the local MES could already represent the aggregation of several other systems, for example, a factory or a town, depending on the resolution and purpose of the study. As will be widely explored here, and from the authors' extensive previous work in this area, DMES flexibility may, for example, refer to the possibility of accessing relatively cheap forms of storage (e.g., from thermal inertia in "smart buildings" [8], [9] or thermal storage (TS) that enables the optimal operation of "smart districts" and "smart communities" [10], [11]), enabling more flexible operation and planning of distributed multigeneration plants [12]–[14], allowing advanced active network management via "power-to-heat" [15], [16] or "power-to-gas" [17], [18] options, and so on.

B. Power System Flexibility

Power system flexibility, particularly looking at the potential contribution from the demand side and DER, can be broadly defined as "the technical ability of a system to regulate the power exchange with the (electricity) grid" [19]. A more detailed but still broad definition is provided in [7], where flexibility is defined as the "ability of a system to provide a secure and economical supply–demand balance across spatial and temporal scales, by leveraging and seamlessly coordinating various controllable assets." Furthermore, focusing on the technical aspects of flexibility, it may useful to distinguish between two forms of flexibility, namely, steady-state and dynamic flexibility, whereby steady-state flexibility is associated with the ability to operate within certain feasible operating regions (FORs) based on steady-state constraints [20], while dynamic flexibility also introduces temporal aspects and constraints (basically related to how fast a new operating point (OP) can be reached, for how long the operation can be sustained, and what is the notice time to carry out the action) [20], [21]. The modeling presented in [22] through the so-called "flexibility triad" noticeably addresses temporal aspects (though not addressing the notice time issue), linking, in particular, the duration of service to be provided with energy availability and constraints (for instance, in energy storage). In [23], the flexibility a power system could deploy some time steps later than a given time is characterized by using flexibility envelopes or cones. The milestone paper [19] outlines key aspects of power system flexibility in the context of aggregation, by using Minkowski summation to build a graphical polytope representation of the flexibility available from multiple aggregated resources, looking at the capacity-ramp-energy flexibility triplet from the abovementioned data [22]. On the other hand, a key aspect that has not been sufficiently studied is the role of networks, in terms of both enabling flexibility and constraining flexibility. In this respect, Wang *et al.* [20] discuss the importance of electricity network constraints in redefining the FORs of an aggregation of DER. However, in none of those works, there is an appreciation for modeling and the role of multienergy resources and MES, a definition of multienergy flexibility, and the potential for DMES to provide flexibility to the power system.

C. Multienergy System Flexibility

The authors first defined what is effectively electricity grid flexibility from DMES in [12] through the concept of electricity shifting potential, which was defined as the "maximum reduction in the electricity input from the electricity distribution system that can be obtained starting from a given initial operational state" of an MES, subject to the relevant multienergy operational constraints. Relevant analytical formulas for such DMES flexibility were also developed for noticeable cases of trigeneration systems. In a similar way, Hinker *et al.* [24] define operational flexibility in MES as the "technical ability of an MES to modulate a certain power feed-in to the grid and/or power out-feed from the grid over time while other power vectors

and resources are ascertained to remain within given boundary conditions." However, the abovementioned definitions only take the (of course crucial) view of flexibility from/to the power system. More generally, and also based on the other considerations made earlier, MES flexibility is defined here as the technical ability of a system to regulate multienergy supply, demand, and power flow subject to steady-state and dynamic constraints and while operating within predefined/desired boundary regions for certain energy vectors. In this respect, it is important to notice that MES OPs and regions belong to a multivector space and are therefore mathematically defined by multidimensional arrays. Depending on the specific use case, it may be convenient to define flexibility of an individual energy vector (of course with electricity as the key reference) while setting certain operating regions and boundaries for the other energy vectors, which leads back to what defined in [12] and [24]. It is also important to notice that, in analogy with the discussion on power system flexibility, also when looking at MES, there is little work that clearly considers and models energy networks. For example, Clegg and Mancarella [25] discuss integrated electricity and gas flexibility concepts, modeling, and metrics, underscoring how gas network constraints can affect electricity system operation. However, there is a lack of systematic discussion on the general role of multienergy networks in enabling or constraining flexibility.

D. Paper Scope and Outline

There are large gaps associated with the concepts of MES and DMES flexibility, and significant challenges arise in terms of the complexity needed to model such flexibility in an appropriate way. Therefore, the aim of this work is to provide a comprehensive overview of technical flexibility assessment of MES and, more specifically, DMES, with a focus on their potential to provide support to a low-carbon grid. To do this, Section II presents key modeling aspects to deal with DMES by introducing the new concept of "multienergy node" as an extension and integration of the concepts of "energy hub" [26], [27] (to deal with DMES) and "power node" [28] (to deal with flexibility) and highlight multiple forms and key features of MES flexibility. Section III, after providing and formulating general definitions of MES and DMES flexibility, introduces a graphical modeling framework, based on multidimensional maps, which are suitable to describe the multivector flexibility characteristics of individual MES. Section IV presents the proposed framework to aggregate multienergy flexibility in DMES. Feasibility and flexibility concepts are applied in Section V to exemplify and discuss specific cases of MES flexibility for a simple system, considering the aggregation of different components and the interactions with the grid, including how multiple energy networks can enable or constrain flexibility. Section VII concludes this article by discussing the next steps and challenges for practical deployment of DMES flexibility.

II. MODELING FRAMEWORK FOR MES FLEXIBILITY APPLICATIONS: FROM ENERGY HUBS AND POWER NODES TO "MULTIENERGY NODES"

A. MES Components

There are number of components that are of particular interest and relevance in DMES studies. The most noticeable family is of course cogeneration or combined heat and power (CHP), which produces both electricity and heat from a unique source of fuel. There are several and complex CHP technologies and plant schemes available [29]. For the relatively small-scale applications of particular interest here (order of below 10 MW_e), diesel and gas engines are the most adopted ones, while fuel cells fuelled on gas or hydrogen are seen as promising applications. Cogeneration plants are also usually accompanied by auxiliary boilers (ABs), supplied by different fuels (including electricity) case by case, for top-up and/or backup purposes. The fuel-based AB is also the reference technology for the production of heat[1] and is usually present as a backup in most plants. Of increasingly important role is the electric heat pump (EHP), which can be of different scales, from individual houses to buildings and districts. EHPs use electricity to move heat from a colder source (e.g., outdoor air, water, or the ground, in the so-called air-source, water-source, and ground-source EHPs, respectively) to a hotter sink (internal environments to be heated). However, they can normally also operate as chillers, as in most air-source heating, ventilation, and air conditioning (HVAC) systems used in buildings. Moreover, electric chillers produce cooling energy (usually through chilled water) based on electricity input and may also have condenser heat recovery options that may be used for cogeneration of cooling and heating [30]. Cooling energy can also be generated by absorption chillers that are fed on exhaust heat in the form of hot water (single-effect) or steam (double- and triple-effect), as well as direct-fired from gas [31]. Absorption chillers are particularly important in the context of trigeneration, which is the extension of cogeneration to include cooling in the so-called combined cooling, heat, and power (CCHP) plants. A technology that is recently gaining extreme importance is also electrolysis, which uses electricity (typically coming from RES) to supply different equipment (such as alkaline and proton exchange membrane electrolyzers) to produce hydrogen from water splitting [18]. The hydrogen produced can be used directly as a fuel, or is further transformed into other fuels, including methane through the Sabatier methanation process [32], [33], or various chemical products such as ammonia [34], [35] or methanol [36].

In this article, we will focus on the characteristics and flexibility aspects of DMES technologies that interact

[1]In "classical" cogeneration studies [29], fuel boilers are the reference technology for the so-called SP of heat, while the SP of electricity happens in the grid itself. SP of course refers to the same useful energy outputs as in the "integrated" electricity-heat cogeneration that takes place in CHP plants.

through electricity, heat, and fuels. For further technologies, particularly for integrated electricity-heat-cooling systems, interested readers can refer to [37], while flexibility studies on trigeneration plants can be found in [12].

B. Local MES Model

For a local MES, the energy hub model is an established framework that can be used as a reference to represent all the energy flows inside the MES and at the external connections [38]. This framework was developed within the project "Vision of Future Energy Networks" [26], started in 2002, and focused on the long-term evolution of the energy systems (for a time horizon of 30–50 years), whereas the energy system structures were fundamentally revisited in a greenfield view, without considering the limitations provided by the current constraints. In the energy hub framework, multiple energy vectors are converted, conditioned, and stored in centralized "energy hubs," which are basically a modeling representation of the local MES plants that incorporates the characteristics and constraints of the available technologies, as well as the connections among these technologies.

Based on the general energy hub concepts and following the authors' work in [39], the local MES can be represented as an input–output gray-box in a matrix model that contains topological and technical conversion data starting from base efficiency features of the constituting components. More specifically, for each plant component $y \in \mathbf{Y}$, where $\mathbf{Y}$ is the set of components in the local MES plant, let us consider the input power in a given time step (in practice, the average power corresponding to the relevant energy associated with that time step) for all the K energy carriers that are involved in the analysis, and let us include these energy carriers in the input array $\mathbf{v}_i^{(y)}$ of dimension $(K \times 1)$. Likewise, the component's power outputs are included in the $(K \times 1)$ array $\mathbf{v}_o^{(y)}$. For every component, a $(K \times K)$ efficiency matrix $\mathbf{H}^{(y)}$ can then be defined which links the input array $\mathbf{v}_i^{(y)}$ and the output array $\mathbf{v}_o^{(y)}$ in the form $\mathbf{v}_o^{(y)} = \mathbf{H}^{(y)}\mathbf{v}_i^{(y)}$.

Examples of efficiency matrices for different components are provided in the Appendix. For the entire local MES plant, a topological representation can then be created through the so-called dispatch factors that describe how each output energy vector from a given component is split into different shares to supply another component, storage unit, demand, etc. [27]. The same type of model can then be constructed for the local MES by considering the input array $\mathbf{v}_i$, the output array $\mathbf{v}_o$, and the overall efficiency matrix $\mathbf{H}$ that links the two arrays, by the relation

$$\mathbf{v}_o = \mathbf{H}\mathbf{v}_i. \tag{1}$$

Note that the above-defined matrices and arrays for both individual components and the whole plant include all the input and output energy vectors, while in general the contents of the input and output arrays for each component and for the MES may be different. Therefore, several elements may be zero. For instance, in the case of energy carriers generated inside the MES but not present as MES inputs, these components are missing (or set to zero in the approach used in [39]) in the input array $\mathbf{v}_i$. Such representation has the advantage of being able to exploit a salient point of the energy hub model, which is that the entries of the overall coupling matrix can be easily found by visual inspection by tracking the connection paths of each energy carrier from outputs to inputs, also including the dispatch factor shares. If all the inputs and outputs are considered to form ordered input and output arrays with the same dimensions, as presented earlier, the overall coupling matrix $\mathbf{H}$ can then be constructed, starting from the efficiency matrices of the individual plant components and from the identification of the topological connections, by using an automatic scheme expressed in symbolic form (see [39] for the details of the algorithm), or with the standardized matrix modeling approach presented in [40].

Another salient point in the modeling concerns the inclusion of different types of energy storage in the energy hub model. More specifically, the matrix model of the storage systems [27] can be set up by considering the storage coupling matrix $\mathbf{S}$, and the array $\dot{\mathbf{e}}$ of the derivatives (approximated by variations) in time of the array $\mathbf{e}$ containing the energy stored for the various energy vectors. As demonstrated in [26] and [41], an interesting and useful aspect is that, after simple mathematical elaborations, it can be appreciated how the contribution of storage to the complete energy hub model becomes additional with respect to the model of the energy hub without storage, regardless of the specific storage location (e.g., upstream or downstream of a conversion device).

In matrix form, the complete energy hub model with storage can, therefore, be simply written as

$$\mathbf{v}_o = [\,\mathbf{H} \quad -\mathbf{S}\,][\,\mathbf{v}_i \quad \dot{\mathbf{e}}\,]^{\mathrm{T}} \tag{2}$$

where the superscript T denotes array transposition, and the variation in time of energy stored in a (discrete) time interval t depends on the difference among the energy stored at the two successive time intervals $t-1$ and t, and on the (nonnegative) energy losses $\mathbf{e}_t^{(\lambda)}$ during time interval t

$$\dot{\mathbf{e}} = \mathbf{e}_t - \mathbf{e}_{t-1} + \mathbf{e}_t^{(\lambda)}. \tag{3}$$

By comparing (1) and (2), it can be clearly seen how storage contributes to plant flexibility by adding further degrees of freedom, considering that the elements of the array $\dot{\mathbf{e}}$ can generally be used as control variables. Additional options have been modeled: the load shifted for demand-side management has been included in the energy hub model as a further additional contribution in [42],

and the energy supply uncertainty depending on customer choices (when alternative solutions are available) has been incorporated in [43].

Further general modeling considerations that are important for the modeling of flexibility refer to ON/OFF operation of plant components such as engines, turbines, etc., which require binary variables. More specifically, following the ideas originally introduced in [44], let us consider a set of binary variables that models the unit commitment of the generic component y in such a way that $b_t^{(y)} = 1$ if y is operating at time interval t, $\overline{b}_t^{(y)} = 1$ if y gets started up at the beginning of time interval t, and $\underline{b}_t^{(y)} = 1$ if y gets shut down at the beginning of time interval t. The ON/OFF status of the unit y at any time interval t will, therefore, obey the following constraint:

$$\overline{b}_t^{(y)} - \underline{b}_t^{(y)} - b_t^{(y)} + b_{t-1}^{(y)} = 0. \tag{4}$$

Furthermore, in order to prevent simultaneous start-up and shut-down of the component y, the following constraint is applied:

$$\overline{b}_t^{(y)} + \underline{b}_t^{(y)} - 1 \leq 0. \tag{5}$$

C. "Multienergy Node" Formulation

Based on the general concepts discussed in Section I-C, and elaborating further on the authors' work in [45], we now present a local MES mathematical model that can be used to develop a suitable flexibility representation.

It is possible to highlight the flexibility aspects of the formulation by rewriting (2) as

$$\mathbf{S}\,\dot{\mathbf{e}} = \mathbf{H}\,\mathbf{v}_i - \mathbf{v}_o = \mathbf{H}\,\mathbf{v}_i - \boldsymbol{\xi} - \mathbf{w} \tag{6}$$

where for convenience, we have used a demand-side sign convention[2] for the array of energy outputs $\mathbf{v}_o$, which has been further broken down into $\boldsymbol{\xi}$, the array of net multienergy process demand (negative if local generation is larger than demand), and $\mathbf{w}$, the array of net enforced energy losses (positive if referring to unserved multienergy demand, and negative if referring to the spilled energy that is supplied locally). Namely, for the sake of clarity, these two arrays that constitute $\mathbf{v}_o$ can be further described as follows:

$$\boldsymbol{\xi} = \mathbf{v}_d - \mathbf{v}_{\mathrm{RES}}; \quad \mathbf{w} = \mathbf{v}_d^{(c)} - \mathbf{v}_{\mathrm{RES}}^{(c)} - \mathbf{v}_o^{(c)} \tag{7}$$

where $\mathbf{v}_d$ is the array of demanded multienergy vectors; $\mathbf{v}_{\mathrm{RES}}$ is the array of locally generated renewable energy in multivector form, e.g., PV or solar thermal; $\mathbf{v}_d^{(c)}$ is the array of multienergy load shedding (unserved multivector energy demand); $\mathbf{v}_{\mathrm{RES}}^{(c)}$ is the array of locally generated renewables that are curtailed; and $\mathbf{v}_o^{(c)}$ is a generic array of energy output that is curtailed (e.g., excess heat produced in cogeneration as a by-product of electricity generation).

[2]Basically, an input/output energy vector is positive when it enters/exits the MES or a component, respectively.

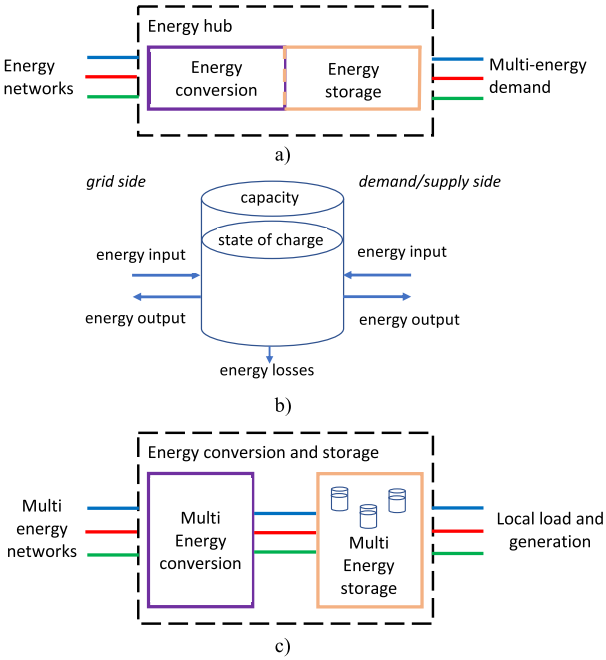

Fig. 2. *From energy hub and power node to multienergy node. (a) Sketch of the energy hub. (b) Power node for the storage system (adapted from [28]). (c) Multienergy node.*

If the analysis is limited to electricity only as the energy vector of interest, and considering that $\mathbf{v}_i$ could be, for instance, conventionally written explicitly considering electricity that is withdrawn from (>0) or injected into (<0) the grid, relation (6) reduces to the well-known power node model used for electrical flexibility assessment [28].[3] Hence, (6) can be effectively considered a multienergy generalization of the power node model, which we thus call here "multienergy node" model (see Fig. 2).

Given the sign conventions used, all components of $\boldsymbol{\xi}$ and $\mathbf{w}$ in (6) are nonnegative, while the following further constraints also apply, as in [19] for the electricity only case:

$$0 \leq \xi_k \cdot w_k \tag{8}$$

$$0 \leq |w_k| \leq |\xi_k| \tag{9}$$

that is, for each energy vector k, local supply or demand and their curtailment need to have the same sign, and

[3]In fact, in order to highlight our modelling extension, we have purposely used the same notation $\boldsymbol{\xi}$ and $\mathbf{w}$ as in [19] to indicate net energy demand and enforced energy losses, while the standing loss components in our formulation are embedded in the storage (3). Other differences relative to the power node model formulation refer to the sign conventions used, which in our case refer to the energy hub model's ones.

supply/demand curtailment cannot be greater than supply/demand itself.

D. Multienergy Node Operational Constraints

The multienergy node model synthesized in (6) is subject to a number of operational constraints, which again are a generalization of the constraints presented in [19], and which generally apply at the level of each component y of the local MES and the whole MES plant itself. In the following, for the sake of simplicity, only the whole-plant modeling will be presented (thus, dropping the subscript y), unless specifically required.

Capacity constraints are generally modeled as lower and upper limits of the output (10), input (11), and storage (12) energy vector flows and of the energy storage capacity (13)[4]

$$\underline{\mathbf{v}} \le \mathbf{H}\mathbf{v}_i \le \overline{\mathbf{v}} \tag{10}$$

$$\underline{\mathbf{v}_i} \le \mathbf{v}_i \le \overline{\mathbf{v}}_i \tag{11}$$

$$\underline{\dot{\mathbf{e}}} \le \dot{\mathbf{e}} \le \overline{\dot{\mathbf{e}}} \tag{12}$$

$$\underline{\mathbf{z}} \le \mathbf{e} \le \overline{\mathbf{z}} \tag{13}$$

Furthermore, intertemporal limitations in changing operational setpoints due to ramp constraints may become particularly important in terms of modeling dynamic flexibility, for example, to provide ancillary services [21]. In this respect, again following the unit commitment binary variable-based modeling approach of [44], specific formulations of the upper and lower capacity limits for plant components with ON/OFF operation need to capture ramp-rate limits[5] for ramp-up and ramp-down (indicated by the arrays $\overline{\mathbf{r}}^{(y)}$ and $\underline{\mathbf{r}}^{(y)}$, respectively) and for start-up and shut-down (indicated by the arrays $\overline{\mathbf{s}}^{(y)}$ and $\underline{\mathbf{s}}^{(y)}$, respectively), as follows:

$$b_t^{(y)}\underline{\mathbf{v}}^{(y)} \le \left(\mathbf{H}^{(y)}\mathbf{v}_i^{(y)}\right)_t \le \left(b_t^{(y)} - \underline{b}_{t+1}^{(y)}\right)\overline{\mathbf{v}}^{(y)} + \underline{b}_{t+1}^{(y)}\underline{\mathbf{s}}^{(y)} \tag{14}$$

$$- b_t^{(y)}\underline{\mathbf{r}}^{(y)} - b_t^{(y)}\underline{\mathbf{s}}^{(y)} \le \left(\mathbf{H}^{(y)}\mathbf{v}_i^{(y)}\right)_t - \left(\mathbf{H}^{(y)}\mathbf{v}_i^{(y)}\right)_{t-1}$$

$$\le b_{t-1}^{(y)}\overline{\mathbf{r}}^{(y)} + \overline{b}_t^{(y)}\overline{\mathbf{s}}^{(y)}. \tag{15}$$

The practical interpretation of (14) and (15) is that the actual upper capacity limit for a specific component y at a given time interval t may be smaller than $\overline{\mathbf{v}}^{(y)}$ if any of the shut-down ramp-rate constraint (the component has to be shut down at next time interval $t+1$), the start-up ramp-rate constraint (the component has to be started up at time interval t), or the ramp-up rate constraint (the component is already in operation at time interval t) is active. Similarly, the actual lower capacity limit at a given time interval t may be smaller than $\underline{\mathbf{v}}^{(y)}$ due to the ramp-down rate (if the component is already in operation at time interval $t-1$) or to the shut-down ramp rate (if the component is being shut down at time interval t).

Further constraints concerning storage operation and relevant to flexibility modeling may also apply depending on the specific case, for example, whereas minimum levels of stored energy capacity are imposed at the beginning and at the end of the analysis period, or such initial and final energy levels must be the same.[6]

III. FLEXIBILITY FROM LOCAL MES

A. General Aspects of Local MES Flexibility Representation

In order to analyze the potential of flexibility of a local MES, it can be considered that the coupling matrix $\mathbf{H}$ is generally noninvertible and the system of equations that describe the energy flows in the local MES is typically undetermined. Under these conditions, the entries of the dispatch factors array $\boldsymbol{\delta}$, therefore, may be used as decision variables in the formulation of optimization problems (and hence in the outlook of providing flexibility in broad terms), in addition to further variables that represent input energy flows to the MES or to individual plant components, necessary to represent nonconstant partial-load efficiencies [39]. In the illustrative example given in [38] for the optimal dispatch of interconnected energy hubs with constant coupling matrix, the minimization of the energy costs with the application of the Karush–Kuhn–Tucker optimality conditions provides the locational marginal costs of the different energy carriers (electricity and heat in the specific case) at each energy hub.

A detailed analysis of the link between the rank of the coupling matrix and the MES flexibility is provided in [46], based on a linearized formulation of the energy hub. Starting from the classical energy hub model, the array of dispatch factors $\boldsymbol{\delta}$ is merged with the input array $\mathbf{v}_i$, and the array $\boldsymbol{\tau}$ of intermediate variables is merged with the output array $\mathbf{v}_o$. The relation between the merged arrays is given by an augmented coupling matrix, such that (example without storage)

$$\begin{bmatrix} \mathbf{v}_o \\ \boldsymbol{\tau} \end{bmatrix} = \begin{bmatrix} \mathbf{H} & \mathbf{H}_{o\delta} \\ \mathbf{H}_{\tau i} & \mathbf{H}_{\tau\delta} \end{bmatrix} \begin{bmatrix} \mathbf{v}_i \\ \boldsymbol{\delta} \end{bmatrix}. \tag{16}$$

The MES flexibility is then linked to the degrees of freedom given by the rank of the matrices $[\mathbf{H}\ \mathbf{H}_{o\delta}]$ and $\mathbf{H}_{o\delta}$.

[4] In addition, for each electricity component, relevant constraints link active and reactive power through the apparent power A, with $P^2 + Q^2 = A^2$.

[5] While, for the sake of generality, we present here the limits as referred to any energy vector, in practice, these limits would only likely apply to an energy vector subset, so that simplified representations could be considered. Furthermore, as different energy vectors are characterized by different time constants, it is possible that for specific studies, ramp constraints may only apply to one energy vector (e.g., electricity, given its generally faster time scales) while the others are assumed to be in steady-state conditions.

[6] Further operational constraints may also refer to the minimum duration of the ON/OFF state of specific components, which typically apply to the operation of relatively large conventional thermal generation units. Given the focus on small-scale DER and DMES here, for the sake of simplicity, we neglect these constraints. The interested reader is referred to [45] for more details on the implementation of these constraints.

B. Multienergy System Flexibility: General Definition, Modeling, and Considerations

Looking at the linear form of the power node formulation, one can directly describe the operation of the system under study with respect to the power exchanged with the grid and have a closed-form representation for electrical flexibility as a feasible deviation in the power exchanged with the grid from the incumbent setpoint.

These simple and intuitive ideas could be extended to the multiple energy vector case by looking at the interface with the external energy networks and the flexibility that an MES can provide by modifying its input energy vectors in the array $\mathbf{v}_i$. However, differently from the electricity-only flexibility case presented in [19], with noninvertible $\mathbf{H}$, it is not possible to write a matrix expression that explicitly represents $\mathbf{v}_i$, which instead is generally expressed as

$$\mathbf{v}_i = \mathbf{v}_i(\mathbf{H},\ \mathbf{S},\ \dot{\mathbf{e}}, \boldsymbol{\xi}, \mathbf{w}) = \mathbf{v}_i(\mathbf{H},\ \mathbf{S},\ \mathbf{x}) \tag{17}$$

where $\mathbf{x}$ is the array of system control variables, defined as

$$\mathbf{x} = \left[\mathbf{v}_i^{\mathrm{T}}, \boldsymbol{\delta}^{\mathrm{T}}, \dot{\mathbf{e}}^{\mathrm{T}}, \mathbf{w}^{\mathrm{T}}\right]^{\mathrm{T}} \tag{18}$$

which generally includes, besides $\mathbf{v}_i$, the dispatch factors $\boldsymbol{\delta}$, the multienergy storage charge/discharge flows $\dot{\mathbf{e}}$, and the potential local multienergy supply/demand curtailment $\mathbf{w}$. It is then possible to define a multienergy flexibility array

$$\boldsymbol{\Phi} = \left[\boldsymbol{\Phi}^{(+)^{\mathrm{T}}}, \boldsymbol{\Phi}^{(-)^{\mathrm{T}}}\right]^{\mathrm{T}} \tag{19}$$

that contains all feasible upward (+) and downward (−) variations $\Delta v_{i,k}$ for each input energy vector k, that is, $\boldsymbol{\Phi}^{(+)} = \{\Delta v_{i,k}^{(+)}\}$ and $\boldsymbol{\Phi}^{(-)} = \{\Delta v_{i,k}^{(-)}\}$. To determine the variations, the multienergy node constraints presented in Section II-E are applied, including, if relevant, intertemporal constraints such as ramp-rate limits, start-up times, and so on.

In practical applications, as discussed in [24], it might be of interest to assess the flexibility of one or two energy vectors at a time while the others are maintained within their feasible region or predefined operational constraints such as to cover a given multienergy demand while responding to an upstream request by the system operator [12]. In the formulation given in Section II-E, this may be carried out by simply setting specific numerical values for $\underline{\mathbf{v}}, \overline{\mathbf{v}}, \underline{\mathbf{v}_i}, \overline{\mathbf{v}}_i, \underline{\dot{\mathbf{e}}}, \overline{\dot{\mathbf{e}}}, \underline{\mathbf{z}}, \overline{\mathbf{z}}$, in the operational constraints (10)–(13), so as to define the FOR as desired in the specific use case.

In general, the flexibility for one given energy vector is a function of all energy vectors via the general multienergy node equations. Thereby, an MES may feature more flexibility than an electricity-only system, given the larger number of variables. More specifically, there are a number of degrees of freedom (i.e., flexibility variables) that can be deployed to provide flexibility, and in general the same new operational point may be reached via multiple paths, for example, by changing the input energy vectors $\mathbf{v}_i$ and/or the plant internal dispatch modeled through the dispatch factors $\boldsymbol{\delta}$ in different ways, which also paves the way to optimization options.[7] This is called energy-vector arbitrage, as already presented in [12], and applies both externally to the MES (e.g., arbitraging across $\mathbf{v}_i$ between electricity and fuel in a dual-fuel heating system with heat pumps and boilers [16], [47]) and internally (e.g., arbitraging, by modulation through $\boldsymbol{\delta}$, between CHP, heat pumps, and boilers to produce electricity and heat [48]). It is thus once again clear how the possibility of modulating the control variables in different ways through different multienergy components and interconnections while meeting the given constraint may be a great source of flexibility that is enabled by the multienergy interaction.

In addition to energy-shifting flexibility, further flexibility options that an MES can enable include multienergy storage arbitrage through the control variable $\dot{\mathbf{e}}$ (including power-to-X options [49]), and two types of curtailments through the control variable $\mathbf{w}$. The first type of curtailment refers to multienergy demand (e.g., curtailing a thermal service by changing the operational setpoints of an HVAC system, which affects the indoor temperature of a building). The second type of curtailment concerns local supply (e.g., by curtailing local PV supply in the case of extra generation). Curtailment is assumed to be a flexibility measure when it comes from a decision taken inside the MES and when no constraint referring to acceptable system operation (including technical operation of the equipment or comfort constraints) is exceeded. Further MES flexibility features are discussed in Section III-E4.

C. Electrical Flexibility From MES

In the context of MES, electricity can be seen as a special case of energy vector, even though with prominent importance due to its high thermodynamic (energy) value, cost, etc. In this respect, and within the general multivector flexibility definition given in Section III-B, electrical flexibility is simply the "technical ability of a plant or component to regulate its exchange of the electrical energy vector with the grid," which is basically the definition given in the earlier section and in [19] and [24]. However, as aforementioned, in MES, one should also define the desired operational constraints in other energy vectors or in case the whole multienergy feasibility region to address specific use cases. Furthermore, a point often overlooked in the context of power system flexibility is the fact that electricity is effectively characterized by two powers, namely, active power and reactive power, and both may obviously play

[7] Presenting an overview of the optimization objectives and tools is not within the scope of this article. The aim of this article is to focus on flexibility modelling and characterization (including visualization). For a conceptual overview of multienergy system flexibility optimization and control, readers may refer to [51]. Optimization aspects and its applications are summarized in [52].

an important role, especially in the context of network and system management [50]. In fact, this is the reason why we bring out active and reactive power explicitly in the multienergy node formulation introduced in Section II-D.

Electrical flexibility is associated with both input active and reactive power deviations.[8] In the context of MES, electrical flexibility may, therefore, be defined as

$$\boldsymbol{\phi}_{\mathbf{e}}(\mathbf{H,S,\ x}) = \begin{Bmatrix} \Delta P_i^{(+)}(\mathbf{H,S,\ x}),\ \Delta P_i^{(-)}(\mathbf{H,S,\ x}), \\ \Delta Q_i^{(+)}(\mathbf{H,S,\ x}),\ \Delta Q_i^{(-)}(\mathbf{H,S,\ x}) \end{Bmatrix} \tag{20}$$

where $\{\Delta P_i^{(+)}, \Delta P_i^{(-)}, \Delta Q_i^{(+)}, \Delta Q_i^{(-)}\}$ is the set of all feasible deviations in the input active and reactive powers from their incumbent values, which depend on **H,S, and x**, and are again subject to the multienergy node constraints presented in Section II-E, including active-reactive power coupling constraints, as well as more specific operational constraints on other energy vectors depending on the specific use case under analysis. It is also important to notice that, in general, the directions of active and reactive power deviations may be different. However, in practical terms when talking about upward/downward electrical flexibility, one would normally refer to the *direction* of the *active* power deviation.

D. "Steady-State" and "Dynamic" Flexibility: Role of Temporal Factors and Constraints

Most literature typically refers to flexibility without addressing temporal issues and focuses on FORs, but without, for example, specifying how long it may take to reach a new setpoint from the current condition. However, as discussed by Mancarella and Chicco [21], temporal aspects may be important when flexibility is relevant to the provision of specific services that are also characterized by the speed of delivery. While this has been generally discussed in [22] with reference to ramp-rate constraints, it had not been practically applied or exemplified in a wide way. A further temporal aspect of interest is related to the duration of the flexibility service delivered. Again, while theoretically mentioned, especially with reference to storage and energy capacity constraints, its practical application has often been overlooked. Another aspect that the authors have explored in [21] is associated with the notice time for the delivery of the flexibility service: this is particularly relevant when there are resources that require a certain start-up or switch-off time, like engines, turbines, CHP plants, etc.

A more complete definition of flexibility, which we call "dynamic flexibility" as opposed to the abovementioned "steady-state flexibility," should, therefore, be characterized by the aforementioned desired temporal features, for example, by expressively indicating the notice time τ_n, the speed of delivery τ_d, and the duration $\Delta\tau$. Hence, focusing on dynamic electrical flexibility, we may write

$$\widehat{\boldsymbol{\phi}}_{\mathbf{e}}(\mathbf{H,S,\ x},\tau_n,\ \tau_d,\ \Delta\tau) = \begin{Bmatrix} \Delta P_i^{(+)}(\mathbf{H,S,x},\tau_n,\ \tau_d,\ \Delta\tau), \Delta P_i^{(-)}(\mathbf{H,\ S,x},\tau_n,\ \tau_d,\ \Delta\tau), \\ \Delta Q_i^{(+)}(\mathbf{H,\ S,x},\tau_n,\ \tau_d,\ \Delta\tau),\ \Delta Q_i^{(-)}(\mathbf{H,S,x},\tau_n,\ \tau_d,\ \Delta\tau) \end{Bmatrix} \tag{21}$$

where the active and reactive power deviations, in addition to the general steady-state operational constraints, are now also associated with the relevant temporal features just discussed. By explicitly introducing temporal features in the flexibility definition, the role of intertemporal constraints for dynamic services also becomes more relevant.

E. MES Flexibility Features and Applications

From the multienergy node formulation and the abovementioned definitions, one can now immediately appreciate all the possible flexibility features and relevant applications of a local MES (see Section IV for further features in a DMES context), provided by the ability to meet a given multienergy demand $\mathbf{v}_d$ by deploying the unique flexibility characteristics, applied to relevant use cases, described in the following.

1) Input Energy Vector Shifting (or Energy Vector Arbitrage): The energy vector arbitrage corresponds to shifting supply across multiple energy vectors in $\mathbf{v}_i$ through the efficiency matrix **H**. There are a number of practical applications of this flexibility feature, which may possibly be considered the key flexibility feature in MES. An important application is, for instance, to carry out price arbitrage across energy vectors, such as based on the spark spread between gas and electricity [53], [54] and while satisfying multienergy demands. Similarly, any flexibility that can be exploited from multifuel devices belongs to this category, for example, in hybrid heat pumps [8], [47] that are based on an EHP and a top-up auxiliary gas boiler for peaking operation: in this case, energy vector arbitrage can be useful to deal with congestions on one supply network, for example, shifting supply from the electrical network to the gas network to satisfy the heat demand [55], [56]. Such energy shifting can also be used in response to ancillary service calls to provide real-time demand response from an MES, as in the applications in [12] where this arbitrage across vectors was introduced via the "electricity shifting potential" indicator.

2) Output Energy Vector Shifting (Power-to-X): Similar to the shifting across input energy vectors described earlier, output energy vectors $\mathbf{v}_o$ can be shifted across as well. A typical example of this flexibility is the whole category of applications generally called "Power-to-X," P2X [49], whereas input electricity, typically from otherwise curtailed renewables, can be transformed, again via the efficiency matrix **H**, into different energy vectors and for various applications. Typically,

[8]Strictly speaking, reactive power is not an "energy vector." However, the general formulation presented here still applies.

the P2X applications include as a starting point Power-to-Hydrogen ($P2H_2$) which may be used in different ways, for example, injection into the gas networks ("Power-to-Gas," P2G [17], [18], if also including methanation), transport [57], production of further clean fuels such as ammonia [58], etc. The other main category is heat "Power-to-Heat," P2H [59], using renewable electricity in heat pumps, electric boilers, etc. Typical use cases include using of excess renewable electricity, to be curtailed because of network constraints or stability constraints, to decarbonize the gas sector [60], [61] (P2G), the heating sector [62] (P2G and P2H), the transport sector [63] ($P2H_2$), various industry sectors (P2X), and so on. Furthermore, when the "X" vectors are easy to store than that of electricity, the P2X energy vector shifting flexibility also enables storing of renewable energy in different forms, as discussed in the following.

3) Temporal Arbitrage via Multienergy (Virtual) Storage: Multienergy storage, like electrical storage, allows exploiting different forms of time arbitrage that may be used for commercial purposes to optimize energy management, reducing peak consumption, and so on. However, what is particularly interesting to highlight in an MES context is how temporal arbitrage on one energy vector through the storage **S** enables flexibility options on other energy vectors via, again, energy shifting considering the coupling matrix **H**. This is, for example, evident in [13], where TS and EHPs enable the enhanced operation and planning flexibility in a CHP plant to optimally participate in energy markets with dynamic prices. Further key applications of multienergy time arbitrage belong to the "virtual" storage [64] category, whereas there is no "physical" storage (e.g., hot water tank); however, for example, the thermal inertia available in the fabric of buildings is used to optimally interact with the electricity system via electro-thermal coupling, providing building-to-grid flexibility and services [8], [9], [65], [66]. Preheating and precooling applications of buildings also belong to this category and rely on virtual storage [67], [68]. In all these kinds of applications, key benefits come from the fact that many flexibility services may be provided at a much lower cost than their counterparts provided by, for example, battery storage.

4) Local Renewable Energy Curtailment: At the local level, RES curtailment $\mathbf{v}_{\mathrm{RES}}^{(c)}$ can be used as a form of flexibility while supplying the local electricity and heat demand. RES curtailment could take place as last resort, for example, and especially to maintain power system stability. In this sense, it may be seen as a sign of a lack of flexibility of the overall power system to which the DMES is connected. In any case, if such a problem could be solved by RES curtailment in one or more MES, this would again point to the flexibility available from DMES.

5) Multienergy Service Curtailment and Comfort Level Arbitrage: An important type of flexibility that can be provided by MES is in terms of service curtailment. In this case, the multienergy array $\mathbf{v}_d^{(c)}$ effectively maps the demand-side energy that affects some form of comfort level and/or quality of service. For example, dimming of lights corresponds to direct electricity reduction and affects somehow the quality of the lighting end-service to the user. More drastically, switching off the supply may provide demand response flexibility at the cost of reliability (see [69]). Moreover, in the multienergy space, changing the setpoints of or switching HVAC systems to provide electricity demand response practically modifies the thermal (heating or cooling) demand profile by not following the user's predefined setpoints, which affects their comfort level [64]. Similarly, the aforementioned exploitation of the building thermal inertia for precooling or preheating arbitrage requires deviations from the user's setpoints. Effectively, these flexibility options correspond to comfort level arbitrage, whereas flexibility in multienergy supply (and eventually electricity, in most cases) is traded off against the comfort level in some energy vector or end-use application. This is usually done for economic benefits for the end-user, so that comfort level requirements may become part of nonfirm multienergy contracts (see [64]). One of the main benefits of this kind of flexibility is that operational constraints are generally easier to relax for other energy vectors (e.g., heat) than electricity, thus again implying that more flexibility even at lower cost may be available in MES.

6) Multienergy Production Curtailment: Similar to local RES curtailment, another flexibility feature that is unique to MES is represented by some form $\mathbf{v}_o^{(c)}$ of energy production curtailment that is carried out to enable operational flexibility for other energy vectors. A typical example is to waste heat produced in cogeneration to allow flexibility in the electricity production for condensation plants, open-cycle gas turbines, and combustion engines whose electricity and heat outputs are tightly coupled by a relatively inflexible cogeneration ratio [37]. Waste heat is an algebraic variable that appears in explicit form only in one equation—the heat balance at the CHP output. As such, it is calculated after having determined the energy balances at the other terminals of the MES components.

7) Relaxation of "Soft" Constraints: This feature corresponds to relaxing, in case only for a limited amount of time, potentially "soft" constraints such as temperature constraints, to create additional flexibility when needed on another energy vectors, for example, for electricity. From a modeling perspective, this can be carried out by simply relaxing the numerical value of the relevant operational constraint of an MES [e.g., $\underline{\mathbf{v}}$, $\overline{\mathbf{v}}$, $\underline{\mathbf{v}}_i$, $\overline{\mathbf{v}}_i$, $\underline{\dot{\mathbf{e}}}$, $\overline{\dot{\mathbf{e}}}$, $\underline{\mathbf{z}}$, $\overline{\mathbf{z}}$, in (10)–(13)] for a certain duration which depends on the impact on the delivery of the final service. For example, in a P2H service, the maximum temperature of heat storage could be increased for some time to allow more energy to be stored under specific conditions.

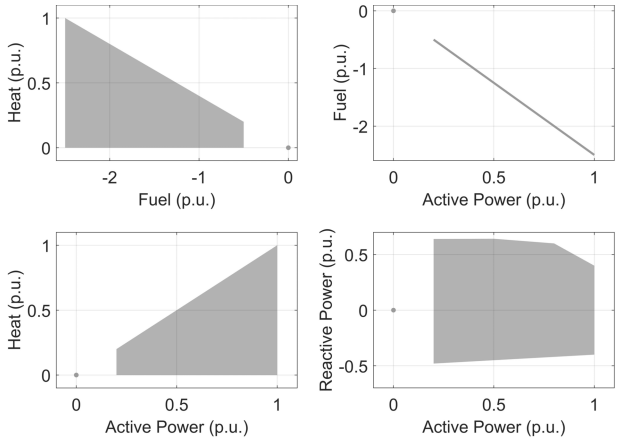

Fig. 3. ***Example of CHP capability/feasibility set for different bidimensional energy vector spaces.***

8) Reactive Power Control to Support (Electrical) Active Power Flexibility: In the context of the flexibility provided to the power system by DMES, a further feature not insofar highlighted in any study comes from the fact that electrical power may actually be broken down into its active and reactive components, so that the DMES model considers active power and reactive power it as if they were two different energy vectors (though linked through their apparent power characteristics and constraints).

Further flexibility features will be presented in the next section with reference to the role of multienergy networks.

F. Visualization of MES Operational Envelopes: Multienergy Flexibility Maps

As discussed in [20], most studies generally describe as (steady-state) flexibility region the FOR of an electrical plant or system. As discussed in [24], similar modeling can be applied to steady-state operational limitations of a component or plant in the multidimensional space of the multiple energy vectors involved in the analysis, for example, electrical active and reactive power, fuel (e.g., natural gas or hydrogen), and heat. The projections of such a multidimensional feasibility or steady-state flexibility region can then be conveniently and efficiently represented onto a bidimensional space of a selected pair of vectors, to describe the capability sets graphically in an intuitive manner.

As an illustrative example, Fig. 3 depicts the capability sets of a CHP plant through (steady-state) "flexibility maps" in the bidimensional spaces "fuel-heat (F-H)," "active power-fuel (P-F)," "active power-heat (P-H)," and "active power-reactive power (P-Q)." All the quantities are expressed in per units based on average power values in a given time step (the terms Heat and Fuel are used for brevity). In the plots, energy vector production is taken with positive sign, while consumption is negative. The CHP plant, in the provided example, is characterized by $P = 1$ p.u. and $H = 1$ p.u., electrical efficiency $\eta_e = 40\%$ and thermal efficiency $\eta_t = 40\%$ (e.g., a diesel engine or a fuel cell), and minimum stable generation (MSG) level equal to 0.2 p.u. Furthermore, it is assumed that the CHP is allowed to spill thermal energy, so that there is a certain flexibility region (in gray) in which the CHP can operate at a given electricity level but for variable heat output, up to the maximum allowed by the P-H characteristic.[9] With these characteristics, at full capacity, the CHP provides 1 unit of heat and 1 unit of electricity by consuming 2.5 units of fuel. For simplicity, linear performance maps with constant efficiencies (and therefore constant cogeneration ratio as well [37]) are assumed for part-load operation, as from the plots.

More in general, "dynamic" flexibility maps could also be considered when subject to temporal limitations, which are represented as subset contained in the temporally unconstrained flexibility regions. For example, by taking again a CHP plant as mentioned earlier, with MSG = 20%, intertemporal constraints for ramp rate equal to 20%/min and start-up time equal to 5 min, Fig. 4 depicts the P-Q flexibility maps considering the CHP starting (left) from 50% loading level, and (right) and from offline (this latter case is equivalent to assuming that the notice time for the flexibility service provision is less than the start-up time). In the figures, it is possible to clearly see the regions that are operationally feasible starting from the considered operational points and subject to the predefined dynamic constraints. It should also be noted that such dynamic maps could be drawn for the multiple energy vectors too, though the different dynamics for the different vectors and relevant components should be modeled appropriately.

IV. AGGREGATING FLEXIBILITY IN DMES

A. Aggregated Multienergy Flexibility in an MES Through Minkowski Summation

The flexibility maps as described earlier are also particularly useful to graphically visualize aggregation of the flexibility provided by multiple resources. In fact, when network constraints are neglected (the impact of networks

[9]It should be noted that if wasting heat is not allowed, for example, due to environmental regulation, the CHP would have no flexibility in varying heat production for a given electricity level as the P-H operational points would be linked by its characteristic line. In this case, thermal storage would be needed to create flexibility.

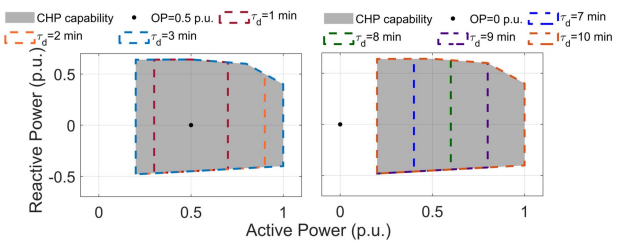

Fig. 4. ***Example of CHP dynamic flexibility in the electrical domain when starting from (left) 0.5 p.u. and (right) offline operation.***

will be discussed in Section IV-B), as shown in [19] for electrical flexibility, the aggregation of the flexibility provided by multiple electrical units mathematically corresponds to add the individual flexibility metrics (which correspond to polytope objects) of each unit through Minkowski summation (represented by the operator $\oplus$).

V. AGGREGATING FLEXIBILITY IN DMES

A. Aggregated Multienergy Flexibility in an MES Through Minkowski Summation

The flexibility maps as described earlier are also particularly useful to graphically visualize the aggregation of the flexibility provided by multiple resources. In fact, when network constraints are neglected (the impact of networks will be discussed in Section IV-B), as shown in [19] for electrical flexibility, the aggregation of the flexibility provided by multiple electrical units mathematically corresponds to add the individual flexibility metrics (which correspond to polytope objects) of each unit through Minkowski summation (represented by the operator $\oplus$).

The concept can be extended to the multienergy case (see [24]) by considering a Minkowski summation across, for example, multiple plant components.

For example, let us consider the following electricity–heat–fuel components with the given nominal characteristics and linear part-load performance map.

1) *CHP:* $P = 1$ p.u., $H = 1$ p.u., $\eta_e = 40\%$, $\eta_t = 40\%$, MSG $= 0$, no waste heat allowed.
2) *AB:* $H = 1$ p.u., $\eta_{\text{AB}} = 100\%$ (a round number is used for simplicity of representation, while the efficiency of modern gas boilers is typically in the order of 80%–90%).
3) *EHP:* $H = 1$ p.u., $COP = 3$.
4) *P2G (Electrolyzer + Methanizer):* $F = 1$, $\eta_F = 50\%$.
5) *TS:* $H = 1$ p.u.

The individual characteristics of these units are shown in the full P-F-H 3-D space and in the F-H, P-F, and P-H 2-D projected planes in Fig. 5.

The plots in Fig. 6 represent all bi-vector operational characteristics of the abovementioned individual components and of various pairwise component combinations, which result in the relevant steady-state FORs for the coupled components. More specifically, the following are observed:

1) This case represents the classical cogeneration case with a CHP plant and a back-up AB.
2) This case illustrates a hybrid heat pump based on EHP and AB (supplied by gas or other fuel).
3) This combination shows a high-efficiency, high-flexibility "virtual CHP plant" with a flexible cogeneration ratio based on the complementarity of CHP and EHP [48].
4) This case shows the coupling between P2G and P2H (based on EHP), which may be suitable in RES-rich areas.

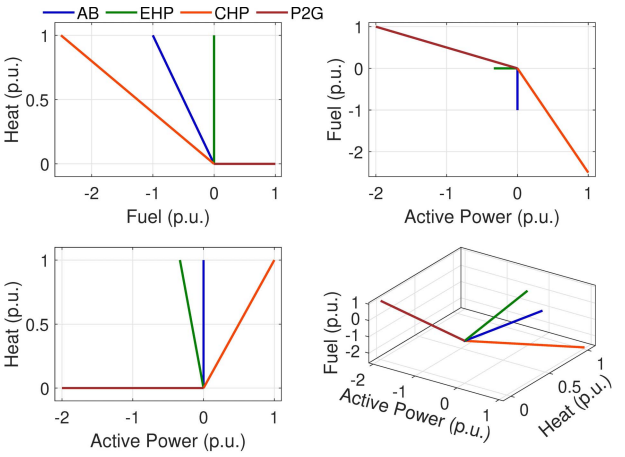

Fig. 5. *Individual operational characteristics of AB, EHP, CHP, and P2G units in (top left) F-H, (top right) P-F, (bottom left) P-H 2-D planes, and (bottom right) P-F-H 3-D space.*

5) This case depicts the effect of coupling a P2G plant with an AB, with potential complementarity in input and output energy vectors.

This example pairs a CHP plant with TS, illustrating how TS can greatly enhance the integrated electricity-heat flexibility through charging and discharging operation.

Fig. 7 shows the polytope that results from the combination of the abovementioned CHP-AB-EHP-P2G units in the P-H-F multivector space, including the bidimensional steady-state flexibility projections for pairwise energy vectors and the flexibility regions for the pairs CHP-AB and P2G-EHP. The overall 3-D polytope and 2-D projections have been obtained by pairing the CHP-AB and P2G-EHP combinations; however, the same results would have been obtained by resorting to other combinations of the four units. The figure clearly shows how the combined flexibility from aggregating multiple MES is greatly enhanced.

B. Multienergy Flexibility in DMES: Networks as Flexibility Enablers

The abovementioned considerations and modeling formulations cover the general case of an MES plant that is aggregating different multienergy components, where the presence of network links is neglected and the focus is on conversion, conditioning, and storage components [70].

This section considers the aggregation of several MES plants and studies the aggregated flexibility of and from such DMES, including the role of networks.

Networks are the means that allow physical aggregation of plants through their energy vectors. For example, the electrical network allows aggregation of electricity supply and demand for different generation plants, load centers, etc. A similar role is played by gas networks or heat networks. As such, it can be said that networks are indeed flexibility enablers. In addition, when several MES plants are brought together via multiple energy networks,

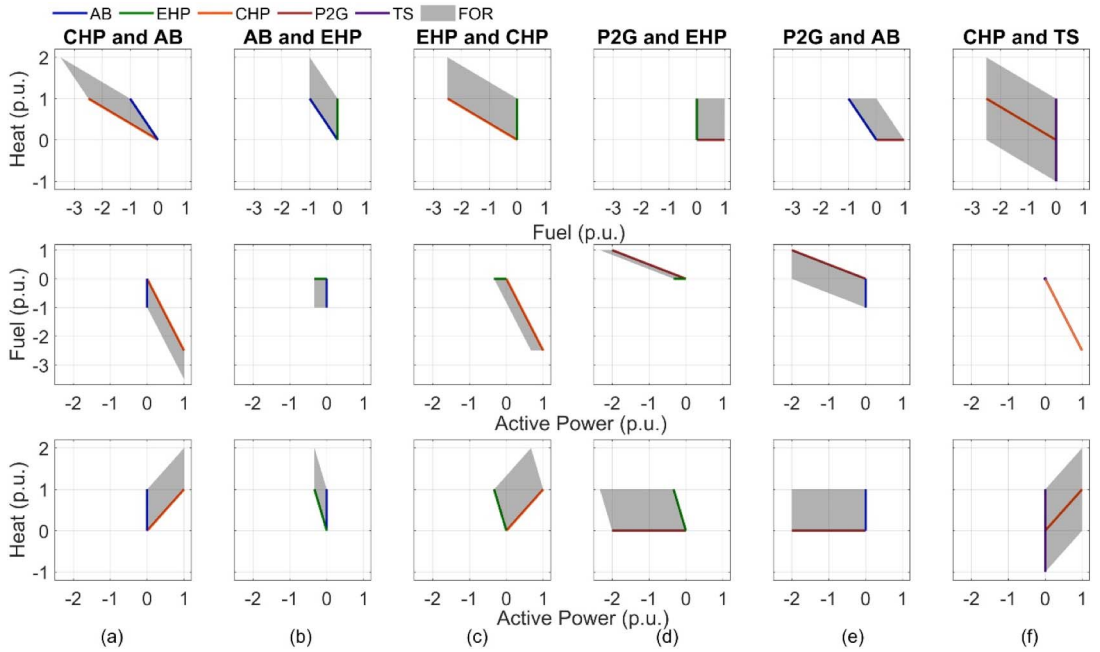

Fig. 6. *FOR in bidimensional spaces (top row) F-H, (middle row) P-F, and (bottom row) P-H for plants formed by different combinations of AB, CHP, EHP, and P2G units.*

not only is flexibility enabled for those energy vectors but also additional flexibility is created/enabled thanks to the cross-vector coupling that is now extended to all multienergy nodes. In practice, the flexibility benefits described earlier from creating an MES plant from aggregating different multienergy components through energy vector coupling (which requires energy vector links, i.e., networks) are now applied and extended to a DMES that aggregates several MES plants. In fact, it is possible to rewrite (19) for the DMES aggregate flexibility of N MES plants as

$$\Phi^{\mathrm{DMES}} = \left[\Phi^{\mathrm{DMES}^{(+)\mathrm{T}}},\ \Phi^{\mathrm{DMES}^{(-)\mathrm{T}}}\right]^{\mathrm{T}} \tag{22}$$

where the entries of the DMES flexibility array, expressed in terms of all feasible upward variations $\Delta v_{i,k}^{\mathrm{DMES}^{(+)}}$ and downward variations $\Delta v_{i,k}^{\mathrm{DMES}^{(-)}}$, for each input energy vector $k = 1, \ldots, K$, and MES plant $n = 1, \ldots, N$, are

$$\Phi^{\mathrm{DMES}^{(+)}} = \left\{\Delta v_{i,k}^{\mathrm{DMES}^{(+)}}(\mathbf{H}_n, \mathbf{S}_n, \mathbf{x}_n)\right\} \tag{23}$$

$$\Phi^{\mathrm{DMES}^{(-)}} = \left\{\Delta v_{i,k}^{\mathrm{DMES}^{(-)}}(\mathbf{H}_n, \mathbf{S}_n, \mathbf{x}_n)\right\}. \tag{24}$$

Subject again to all relevant constraints for all N MES plants. The expressions (21)–(24) confirm how cross-vector flexibility "propagates" beyond the specific energy vectors that are linked through the relevant energy networks.

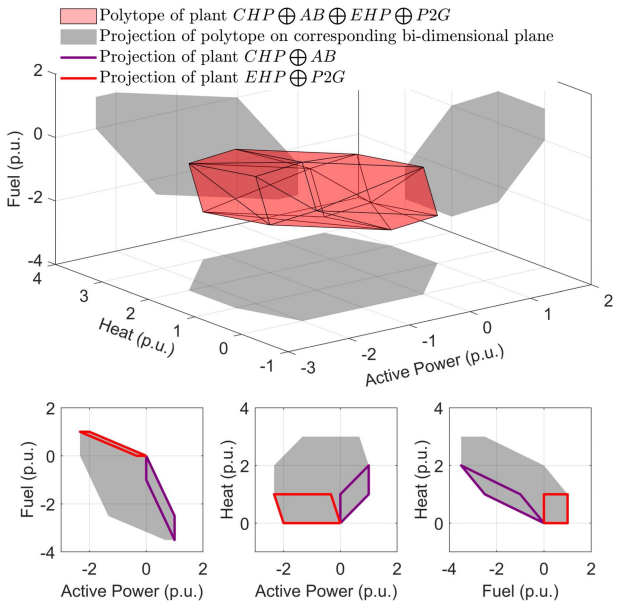

Fig. 7. *Polytope of the FOR of an MES with CHP, EHP, AB, and P2G in the active power, fuel, and heat 3-D space (top) and its projections onto the (bottom left) P-F, (bottom middle) P-H, and (bottom right) F-H 2-D spaces.*

C. Impact of Network Constraints on Multienergy Flexibility

Following the same procedures as mentioned earlier, if network constraints are neglected, the aggregated flexibility of a DMES for a given energy vector can be obtained again via Minkowski summation of the operational maps of each MES for the specific energy vectors for which a

network is available, where the sum is extended to the MES plants (out of the total number of MES plants N) connected through a network for that energy vector.

In a more general (and realistic) case, a network for a generic energy vector k that links multiple MES plants will be subject to physical characteristic constraints (e.g., power flow or gas flow equations) as well as steady-state and dynamic operational constraints (energy transport capacity, min/max voltage or pressure constraints, etc.). Such equality and inequality constraints are in general nonlinear, and their form depends on the specific energy vector, as discussed in [27], also involving other characteristic variables in addition to energy flows, such as voltages, pressures, temperatures, etc. Typical multienergy equations and a generalized Newton–Raphson solution algorithm for integrated electricity, heat, and gas networks can, for example, be found in [71]. A general formulation of network constraints is, therefore, of the form

$$\mathcal{E}(\mathbf{v}_{i,1}, \ldots, \mathbf{v}_{i,N}, \boldsymbol{\theta}) = \mathbf{0}, \quad \beth(\mathbf{v}_{i,1}, \ldots, \mathbf{v}_{i,N}, \theta) \leq \mathbf{0} \quad (25)$$

where $\mathcal{E}$ and $\beth$ are, respectively, the sets of (generally nonlinear) equality and inequality network constraints that link together the N arrays $\mathbf{v}_i$ of input energy vectors at each MES plant in the DMES under consideration, and $\boldsymbol{\theta}$ is a generic set of additional variables required to describe the physical constraints for each network.

In practical applications, as done, for example, when considering dc approximations for the electrical network (e.g., for market operation), one could assume that the generally complex set of nonlinear equations and constraints for multienergy networks which contain multiple types of variables can be reduced to a simpler, approximated set of constraints (in case linear or linearized) that refer to the energy vector power input arrays $\mathbf{v}_i$ for all N MES plants (see [72] and [73]). This approximation is particularly convenient for conceptual analysis as we are carrying out here so that complex network constraints can simply be reduced to constraints on the input or output energy vectors of each plant.

What we would now like to study is the impact of energy network constraints on multienergy flexibility. More specifically, while networks enable aggregation benefits in first place, as discussed earlier, the presence of network constraints will limit flexibility. Mathematically, this is evident given that network constraints may be modeled as constraints to the input arrays $\underline{\mathbf{v}_i}, \overline{\mathbf{v}_i}$ and output arrays $\underline{\mathbf{v}_o}, \overline{\mathbf{v}_o}$ for each plant, where such constraints would generally be more limiting than the base operational/feasibility constraints for the plant. Therefore, some areas of the flexibility regions will no longer belong to a feasible set, and so a feasibility region that is a subset of the previously defined flexibility region will be defined. Furthermore, it will no longer be possible to adopt a vanilla Minkowski summation to build such feasibility regions, and specific algorithms that also involve the detailed energy flow equations will be needed (see [20]). Finally, as a key effect of the presence of network constraints, the overall DMES flexibility region will be segmented into different local flexibility regions due to the presence of constraints even in just one of the energy vectors.

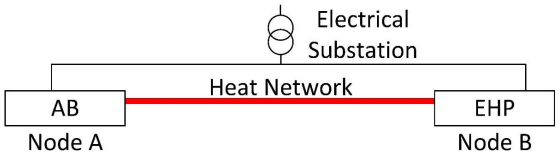

Fig. 8. *Test system 1 to demonstrate the impact of networks on nodal and overall DMES flexibility.*

The abovementioned considerations are illustrated with the canonical example in Fig. 8, where two multienergy electricity–heat demand nodes are connected via an upstream electrical network and directly via a thermal network branch of variable size. The heat supply is assumed to be a gas boiler in node A (the gas network is not depicted) and an EHP in node B. When there is no thermal network, there is no flexibility in this test DMES, as the electrical demand is fixed in all nodes, including in node B to satisfy the heat demand. However, when the thermal link is introduced, the heat demand in each node can be partly fulfilled by both the AB and the EHP, thus generating flexibility in the electrical system, which is a form of energy vector/network arbitrage. This is shown in Fig. 9, where plots are drawn for different heat network capacities ranging between zero and one per unit. It can be clearly seen from the pictures that when there is no thermal link, there is no flexibility available in the DMES as the two nodes are thermally separated, with *P-H* characteristics of the respective components. However, while the thermal branch capacity increases, so does the DMES flexibility,

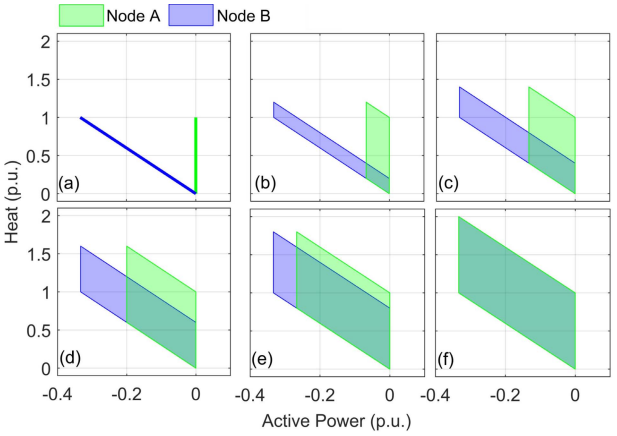

Fig. 9. *Impact of various capacity levels (0–1 at 0.2 intervals, from (a) to (f), respectively) of the connecting thermal network on the P-H flexibility regions of node A and node B.*

up to the point when, for heat network capacity equal to one per unit, a full thermal backup can be provided by one node to the other, corresponding to the full flexibility region of the AB-EHP combination. For intermediate heat network capacities, the two distinct flexibility regions for the two nodes can be clearly appreciated.

D. Multienergy Network-Related Flexibility Options and Constraints

While constrained networks may generally limit the size of the feasibility region, in a DMES context, it is also possible to positively exploit multienergy features of different networks through network-related flexibility options. In particular, three key flexibility options that may be associated with multienergy networks are presented in the following, which add to the flexibility features discussed in Section III-E. Furthermore, the impact of the network constraints on the available multienergy network-related flexibility is also discussed.

1) Energy Network Arbitrage: In this case, in an MES context, if one network is congested, a network for another energy vector could be used to transfer useful energy in some form. For example, power-to-heat could be used to transfer across a heat network zero-carbon heat from renewables that need be curtailed due to electrical network congestion. A similar example for power-to-gas can be found in [17]. This kind of flexibility effectively pairs well with the energy-shifting arbitrage presented in Section III-B, which refers to substitution across energy vectors at the inputs of a plant.

2) Utilization of Network-Embedded Storage: Such examples may refer, for example, to the deployment of thermal inertia from the water in heating and cooling networks to optimize the management of integrated electricity and thermal systems (see [74]), or to the deployment of linepack pressure flexibility in gas networks to deal with electricity constraints [25], [75]. From a modeling perspective, an intuitive way to represent this flexibility option could be to embed a simple storage model into steady-state network equations. However, in practical terms, it may be difficult to identify the parameters of such model and the approximation for complex dynamics such as for gas network might not be satisfactory.

3) Relaxation of Network Operational Constraints: Similar to the relaxation of constraints in some energy vector operation to facilitate overall MES flexibility, it may also be possible to relax some of the physical constraints that characterize multivector network operation, for example, in terms of pressure for gas networks, temperature for thermal networks, water velocity for water networks, etc. (see, e.g., relevant ideas in [76] and [77]). Of course, again this relaxation should still be carried out within acceptable, secure limits and not for a sustained duration. In terms of modeling, in the simplified representation discussed in Section III-B, this flexibility option corresponds to relax the numerical value of the constraints that will eventually apply to the multienergy input arrays of relevant plants.

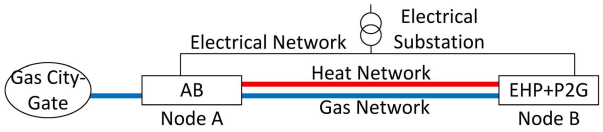

Fig. 10. *Test system 2 to demonstrate multienergy network-related constraints and flexibility features.*

4) Illustrative Examples: To illustrate some of the multienergy network-related effects of constraints and flexibility features discussed, let us consider the test case shown in Fig. 10.

Fig. 11 shows how the FOR of the whole DMES greatly changes (and is enhanced) when multiple networks are added (here assumed unconstrained). This may be particularly useful when the electrical network may be constrained and renewable energy might have to be curtailed (imagine, e.g., RES at node B that cannot transfer electricity due to voltage constraints). Arbitraging across energy networks, e.g., from electricity to heat and/or gas after P2H and/or P2G at node B, may, therefore, be a suitable means to avoid RES curtailment.

The corresponding network-constrained case is then analyzed in Fig. 12, where the effects of the constraints on the flexibility of node A are evident. Even more interesting is Fig. 13, which shows the effects of constraints on the flexibility of both node A and node B. It can be noticed that because of the asymmetric technology present at node A and node B, the flexibility characteristics of both nodes may be (very) different in the case of segmented flexibility regions due to network limits, as aforementioned. For example, electricity can be consumed at node B, converted to gas, and sent to node A via the gas network. However, at node A, there is no P2G, and therefore the abovementioned operation is not possible.

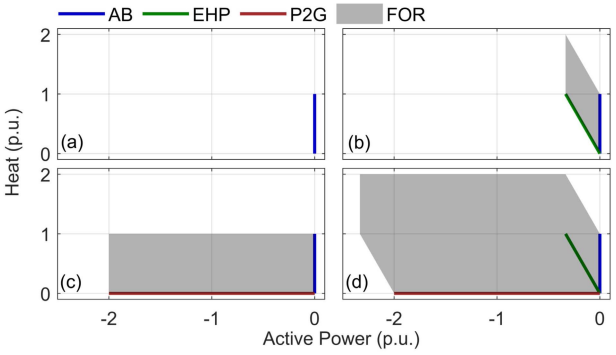

Fig. 11. *Test system 2's node A FOR represented in the P-H plane under (a) no network, (b) only heat network, (c) only gas network, and (d) both heat and gas networks coupling of node A and node B (unconstrained network case).*

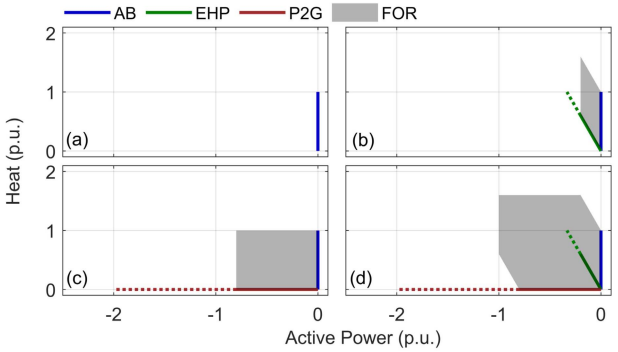

Fig. 12. *Test system 2's node A FOR represented in the P-H plane under (a) no network, (b) only heat network, (c) only gas network, and (d) both heat and gas networks coupling node A and node B (constrained network case: solid lines represent the capacity that can be transferred; dotted lines represent the capacity that is constrained due to networks; network constraints are assumed equal to 0.4 p.u. for gas and 0.6 p.u. for heat).*

Let us now consider the test system 3 shown in Fig. 14 to demonstrate further possible examples of the application of DMES flexibility.

A first use case refers to assessing the electrical flexibility that can be provided by the whole DMES (EHP + AB + CHP + EHP, assuming no network constraint). In this respect, Fig. 15 illustrates the H-P map (left) of the test system and the maximum available active power flexibility against the heat demand level. The flexibility largely depends upon the status of the CHP plant. In particular, when the CHP is offline, the flexibility is much smaller as only the EHP is able to contribute to electrical flexibility by energy vector arbitrage through AB support. It is also evident how the maximum electrical flexibility depends on the operational point (heat demand) and is therefore time-varying, as will be further shown in Section VI.

In addition, the distribution of upward and downward flexibility is also dependent upon the operational point of units with electricity interaction, that is, EHP and CHP. For

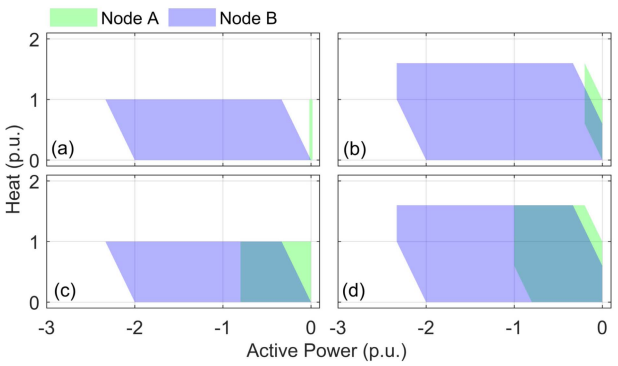

Fig. 13. *Test system 2's P-H FOR of node A and node B for different capacities of heat network for cases with (a) no network, (b) only heat network, (c) only gas network, and (d) both heat and gas networks (constrained network case as aforementioned).*

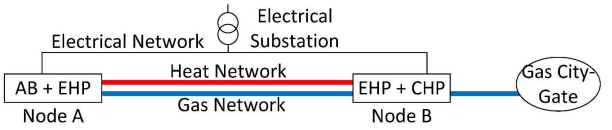

Fig. 14. *Test system 3.*

example, let us assume that the CHP is offline and heat demand is 1 p.u.: this could be either entirely fulfilled through the AB and result in 0.33-p.u. downward flexibility and no upward flexibility, or entirely through the EHP and result in 0.33-p.u. upward flexibility and no downward flexibility. Similar partial fulfillment of the heat load by the AB and EHP would result in both upward and downward flexibility.

From the aforementioned discussion, it is therefore clear that both the heat demand level and the combination of resources, by which heat demand is met, play a crucial role to determine both upward and downward flexibility. In this respect, the upward and downward flexibility of Test system 3 for a heat load of 2 p.u. for an arbitrary combination of resources is shown in Fig. 16(a). Note that the OP can be controlled along the vertical line corresponding to a required heat load equal to 2 p.u. through the combination of EHP, CHP, and AB. This therefore enables potential modulation so as to make both upward and downward flexibility available to the upstream electricity grid, if, for example, there was a call from the system operator to provide a flexibility service. If the heat demand conditions were to be uncertain (as in practical cases), the flexibility that could be provided is in essence the minimal available flexibility over the range of uncertain heat demand, as shown in Fig. 16(b) for a heat load equal to 2 ± 0.25 p.u. of uncertainty. Furthermore, in this case study, one can appreciate how the operating range of flexibility might not be continuous due to the nonconvexity of the system FOR. In this regard, Fig. 16(c) shows that for a heat load of 2.75 p.u. the downward flexibility is

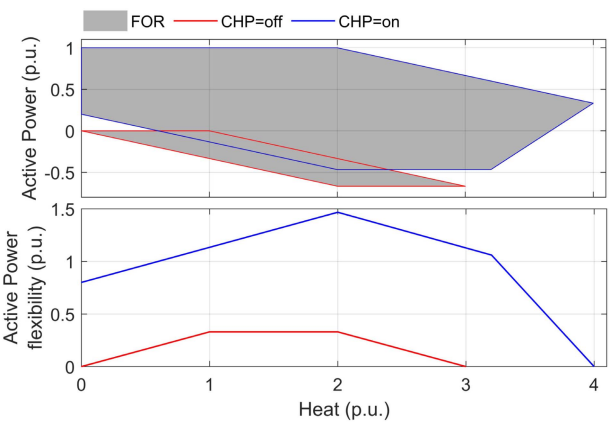

Fig. 15. *FOR in the (top) H-P plane and (bottom) electrical flexibility of test system 3 with CHP ON/OFF.*

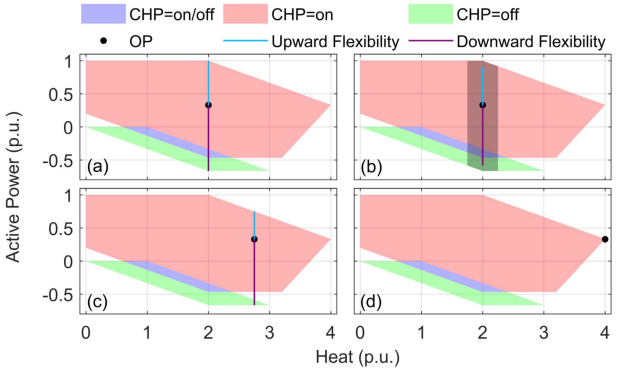

Fig. 16. *Electrical upward and downward flexibility of test system 3 under (a) heat load equal to 2 p.u., (b) heat load equal to 2 ± 0.25 p.u. uncertainty interval, (c) heat load equal to 2.75 p.u. (showing nonconvexity in the FOR due to CHP ON/OFF operation and MSG), and (d) heat load equal to 4 p.u. (showing lack of electrical flexibility in that OP).*

discontinuous while transitioning from the red area to green area, due to switching ON/OFF the CHP and to the presence of an MSG level. Moreover, Fig. 16(d) shows that only one possible combination of resources (i.e., all units are operating at maximum capacity) can be deployed to fulfill a heat load of 4 p.u., and thus the system lacks any electrical flexibility in that particular OP. From this point of view, the dynamic flexibility discussed in Section II-E is particularly important to determine the time required to deliver such flexibility from DMES.

E. Profitability Mapping Onto the Flexibility Region

The technical flexibility discussed in the abovementioned studies and available from DMES can be exploited in different ways. One of these ways is the provision of grid services in response to specific rewards.[10] For this purpose, starting from the current OP, an ideal DMES system manager or aggregator has to assess the possible profits that would come from the participation in the provision of these services. For this purpose, costs and benefits may be mapped against the flexibility region [14]. If the initial DMES OP minimizes the operational costs, any energy shifting from that point to another point belonging to the flexibility region determines extra costs. Conversely, if the initial OP is not cost-optimal, the situation could become even more favorable for the DMES operator when the energy shifting was to be carried out in the direction of further reducing the operational costs. The benefits are generally given from rewards that remunerate the willingness to participate in the provision of the services. The mapping of the profits (given by revenues minus costs)

[10]While this article has focused on technical flexibility, economic/commercial flexibility of MES and relevant benefits are of course another important topic of research. The interesting reader may, for example, refer to [12] and [14] for relevant insights.

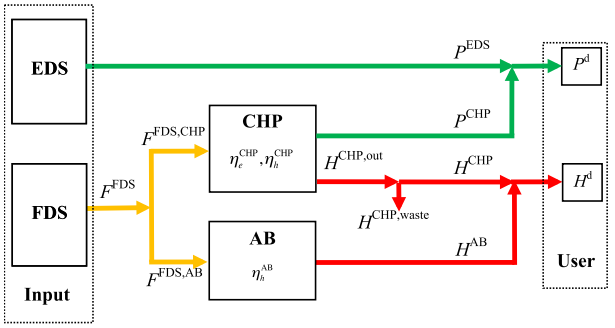

Fig. 17. *Scheme of a simple MES system.*

determined from the difference between costs and benefits onto the flexibility region makes it possible to identify the electricity reduction from the electrical network leading to the maximum profit. Given a reward plan, the conditions of maximum profit occur for a certain average power of electricity shifting that corresponds to the maximum positive distance between rewards and electricity shifting costs. In [14], this average power defines the maximum profit electricity reduction (MPER). An indicative example is shown in Section VI-D. In a market-based context for flexibility services procurement, this electricity reduction may become the quantity offered by, for example, DMES managers or aggregators to the market operator.

VI. ILLUSTRATIVE EXAMPLES ON A CHP-BASED SYSTEM

In order to exemplify the concepts referring to MES flexibility, let us consider a simple system (see Fig. 17) with energy inputs from the electrical distribution system (EDS) and the fuel distribution system (FDS). At the user's side, electrical and heating loads are served through the EDS, the CHP, and the AB. Local energy storage is not represented in this example.

For this system, the individual regions of operation of the system components are known (see Fig. 18), namely, $\boldsymbol{B}^{CHP}$ for the CHP, $\boldsymbol{B}^{EDS}$ for the EDS, and $\boldsymbol{B}^{AB}$ for the AB. In particular, the CHP is of back-pressure type and is characterized by a constant heat-to-power ratio between the

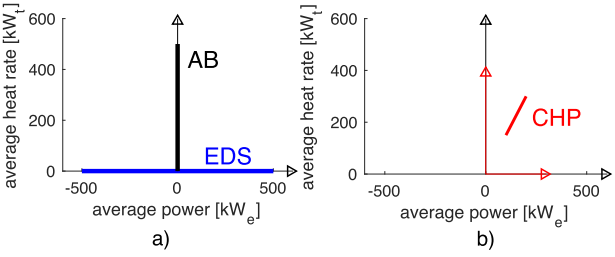

Fig. 18. *Individual regions of operation of the simple MES components. (a) Regions of operation of EDS and AB. (b) Region of CHP operation.*

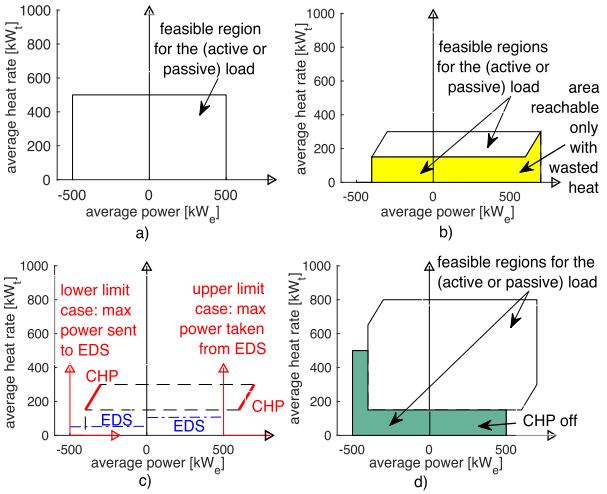

Fig. 19. ***MES capability region to reach the possible electricity and heat demand points. (a) SP from EDS and AB (without CHP). (b) EDS and CHP (without AB). (c) Interpretation of the case without AB. (d) All components, with no wasted heat.***

technical minimum ($\underline{P}^{(\mathrm{CHP})}$, $\underline{H}^{(\mathrm{CHP})}$) and the full output ($\overline{P}^{(\mathrm{CHP})}$, $\overline{H}^{(\mathrm{CHP})}$). The AB has an admissible range from zero to $\overline{H}^{(\mathrm{AB})}$. For the EDS, the limits are given by the apparent power that can be taken from or injected into the EDS; the active power limits ($\underline{P}^{(\mathrm{EDS})}$, $\overline{P}^{(\mathrm{EDS})}$) considered in this example correspond to the minimum and maximum active power determined for a given reactive power. In principle, the limits for the electricity taken from the EDS or injected into the EDS may be asymmetrical, because of grid congestion constraints in the supply network, voltage control actions, or rules imposed to limit the reverse power flows.

The feasibility regions drawn to serve active power and heat demands are obtained by using the Minkowski sums of the individual regions of operation of the components (see Fig. 19). The portion of the region $\boldsymbol{B}^{\mathrm{EDS}} \oplus \boldsymbol{B}^{\mathrm{AB}}$ with positive active power [see Fig. 19(a)] corresponds to the separate production (SP) of electricity (taken from the EDS) and heat (from the AB), without using the CHP. The part of the region $\boldsymbol{B}^{\mathrm{EDS}} \oplus \boldsymbol{B}^{\mathrm{AB}}$ with negative active power may be reached in general in the presence of active demand (i.e., with local electricity generation) at the user's side.

If the AB is off, the capability region $\boldsymbol{B}^{\mathrm{EDS}} \oplus \boldsymbol{B}^{\mathrm{CHP}}$ is shown in Fig. 19(b); the lower area corresponds to the points reachable only by assuming that part of the produced heat may be wasted off to the ambient. For the graphical construction of this capability region, the CHP diagram is "moved" with respect to the EDS region $\boldsymbol{B}^{\mathrm{EDS}}$ from the lower to the upper value [Fig. 19(c) shows the limit cases for the lower and upper P limits, as well as an intermediate situation; this "moving CHP diagram" concept is also used below for further intuitive interpretations]. Finally, the capability region $\boldsymbol{B}^{\mathrm{EDS}} \oplus \boldsymbol{B}^{\mathrm{AB}} \oplus \boldsymbol{B}^{\mathrm{CHP}}$ with all components is drawn in Fig. 19(d) if no wasted heat is allowed. It can be noticed that there is an area reachable only when the CHP is off. If the CHP is on and waste heat is allowed, the area indicated in Fig. 19(c) is partially superposed with the CHP-off area.

A. Flexibility for Fixed Demand

The feasibility region $\boldsymbol{B}^{\mathrm{EDS}} \oplus \boldsymbol{B}^{\mathrm{AB}} \oplus \boldsymbol{B}^{\mathrm{CHP}}$ corresponds to all the multienergy demand points reachable by using the available components in the MES. In order to assess flexibility, it is important to refer to a given OP (with subscript 0). Fig. 20 shows an exemplificative situation with passive demand (i.e., $P^{(d)} \geq 0$ and $H^{(d)} \geq 0$). The electricity demand is assigned to $P_0^{(d)} = 400$ kW$_e$ (average active power in a given time interval) and the thermal demand is $H_0^{(d)} = 600$ kW$_T$ (average heat rate in a given time interval). The point $(P_0^{(d)}, H_0^{(d)})$ cannot be reached from SP, so that all components are needed. Let us consider the "moving CHP diagram" to explain the possible operating conditions in the reference situation shown in Fig. 20(a). The CHP region has to include the demand point. The CHP electrical and thermal generation values are determined from the CHP diagram ($P_0^{(\mathrm{CHP})} = 150$ kW$_e$, $H_0^{(\mathrm{CHP})} = 225$ kW$_T$). The EDS and AB contributions ($P_0^{(\mathrm{EDS})} = 250$ kW$_e$, $H_0^{(\mathrm{AB})} = 375$ kW$_T$) are then determined in a complementary way, with the visual representation indicated in Fig. 20.

In order to assess feasibility, the range of variation of the operational conditions can be found by moving the CHP diagram in such a way that all the points located on the CHP characteristic, from the technical minimum to the full output, pass from the point $(P_0^{(d)}, H_0^{(d)})$. With the

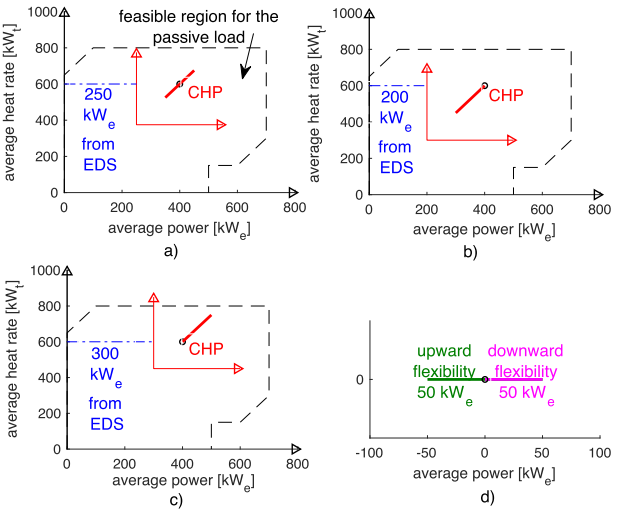

Fig. 20. ***Flexibility region starting from a given electricity and heat demand. (a) Reference case for the usage of the CHP. (b) Maximum reduction in the average power taken from the EDS. (c) Maximum increase of the average power taken from the EDS. (d) Upward and downward flexibility.***

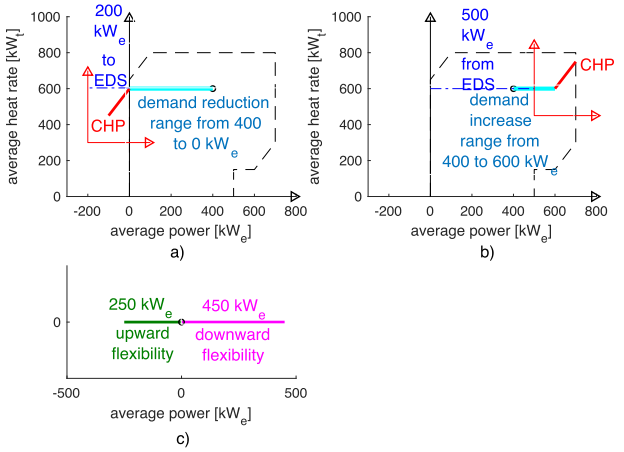

Fig. 21. ***Flexibility region with ranges of curtailable demand and demand increase. (a) Accepted electrical demand reduction. (b) Accepted electrical demand increase. (c) Upward and downward flexibility.***

reduction in the electricity input from the EDS, the limit situation (with subscript 1) occurs when the CHP operates at full output, as shown in Fig. 20(b). The CHP electrical and thermal generation values ($P_1^{(\mathrm{CHP})} = 200$ kW$_e$ and $H_1^{(\mathrm{CHP})} = 300$ kW$_T$) are again determined from the CHP diagram. Correspondingly, $P_1^{(\mathrm{EDS})} = 200$ kW$_e$ and $H_1^{(\mathrm{AB})} = 300$ kW$_T$. The maximum reduction in the active power input is $P_0^{(\mathrm{EDS})} - P_1^{(\mathrm{EDS})} = 50$ kW$_e$. Conversely, if it is needed to increase the electricity input from the EDS, the limit situation (with subscript 2) occurs when the CHP operates at its technical minimum output, as shown in Fig. 20(c). The values for the CHP are $P_2^{(\mathrm{CHP})} = 100$ kW$_e$ and $H_2^{(\mathrm{CHP})} = 150$ kW$_T$, corresponding to $P_2^{(\mathrm{EDS})} = 300$ kW$_e$ and $H_2^{(\mathrm{AB})} = 450$ kW$_T$. The maximum increase of the active power input is $P_2^{(\mathrm{EDS})} - P_0^{(\mathrm{EDS})} = 50$ kW$_e$.

The above-determined conditions are represented in a graph [see Fig. 20(d)] that represents the maximum upward and downward flexibility that can be obtained by changing the way to supply the fixed electricity and heat demand, without considering intertemporal or other constraints. In particular, in this example, these changes are due to the variation of the OP of the CHP, which correspondingly determines the contributions from the EDS and the AB. In summary, the maximum flexibility region $\boldsymbol{\Phi}$ is represented as the union $\boldsymbol{\Phi} = \boldsymbol{\Phi}^{(+)} \bigcup \boldsymbol{\Phi}^{(-)}$ of the region $\boldsymbol{\Phi}^{(+)}$ with a reduction in the active power taken from the EDS and $\boldsymbol{\Phi}^{(-)}$ with an increase in the active power taken from the EDS.

B. Flexibility With Curtailable Demand or Demand Increase

Let us now consider the possibility to change the electrical demand, by keeping the heat demand unchanged, for example, to maintain the same level of comfort for the users. If the demand is curtailed, Fig. 21(a) shows the limit case in which the demand is reduced to zero. In this case, the CHP can be exploited by sending its maximum electrical output (200 kW$_e$) to the EDS. Therefore, the average electric power taken from the EDS changes from 250 kW$_e$ in the reference case to -200 kW$_e$, with a difference of 450 kW$_e$ that corresponds to the maximum downward flexibility. On the other side, Fig. 21(b) shows the limit case in which the average power of the user reaches the maximum feasible value (600 kW$_e$) which is consistent with the maximum average power taken from the EDS (500 kW$_e$) and with the exploitation of the CHP at its minimum output. The maximum upward flexibility, determined as the EDS input increase with respect to the reference case, is 250 kW$_e$, and it is conventionally represented with a negative sign [see Fig. 21(c)].

C. Flexibility for Fixed Demand With Dynamic and Grid-Dependent Limits

The abovementioned feasibility conditions refer to the fact that all the points belonging to the CHP characteristic may be reached at any time. However, in practice, this could not always happen. The presence of limitations to reach the entire region $\boldsymbol{\Phi}$ determines the flexibility of the MES operation. Two cases are addressed in the following, for time-dependent and grid-dependent limitations, respectively.

1) *Time-Dependent (Dynamic) Flexibility Limits*: Considering the evolution of the MES variables during a specific time, with the assessment of the MES operation carried out at successive time steps of duration Δt, the possibility of reaching a given CHP OP depends on the CHP OP at the previous time step, and on the effect of ramp-rate constraints or CHP start-up (in the limit case, the CHP could have been in the off state at the previous time step). Fig. 22 shows

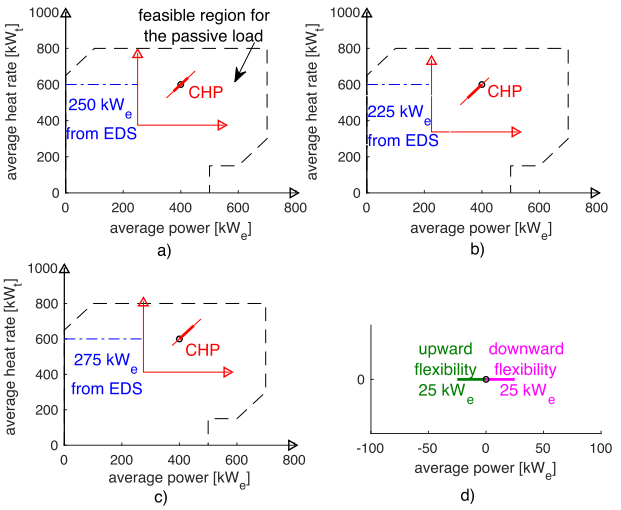

Fig. 22. ***Dynamic flexibility region reduced by time-dependent limits. (a) Reference case for the usage of the CHP. (b) Maximum reduction in the average power taken from the EDS. (c) Maximum increase of the average power taken from the EDS. (d) Upward and downward dynamic flexibility.***

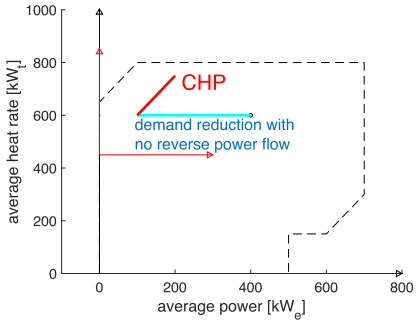

Fig. 23. ***Flexibility region reduced by grid-dependent limits (no reverse power flow).***

an indicative example of CHP characteristics limited by operational intertemporal constraints, in which the shrinking of the flexibility region depends on the ramp-rate constraints or the CHP start-up. The thick line on the CHP characteristic indicates the reduced range of CHP operation, while the thin line is reported to show the remaining unused part of the CHP full range of operation considered at a steady state. The limit conditions for the CHP operation are given in the example by using only 50% of the operational range. The flexibility ranges are determined by applying the same approach shown in Fig. 20.

2) *Grid-Dependent Flexibility Limits:* A limit is imposed on the grid, for example, to avoid the presence of reverse power flow to the grid in the case with curtailable demand. Fig. 23 shows the difference with respect to Fig. 21 when the CHP is used (at its minimum output). The average power taken from the EDS is null so that the downward flexibility is 250 kW$_e$.

D. Indicative Examples of Profitability Mapping Onto the Flexibility Region

Fig. 24 shows two indicative examples of mapping the extra costs (thick lines) and possible reward plans (different cases represented with dashed lines and labeled from A to F for upward flexibility, and from A' to F' for downward flexibility) for changing the OP to provide flexibility services. The extra costs are represented in stepwise form, with steps at ± 10 and ± 30 kW$_e$. In Fig. 24(a), it is assumed that the initial OP is cost-optimal so that any change results in positive extra costs. Conversely, in Fig. 24(b), the initial point is not cost-optimal, so that better conditions with economic savings could occur even when providing some downward flexibility. For example, in the downward flexibility case with the reward plan B', the MPER (as defined in [14]) occurs for 30 kW$_e$ in Fig. 24(a), and 50 kW$_e$ in Fig. 24(b). If the reward becomes sufficiently high (e.g., for the reward plans F and F'), maximum flexibility (called electricity shifting potential in [21]) can be achieved in a convenient manner. However, for relatively low rewards [e.g., with the reward plan A for upward flexibility in Fig. 24(b)], no upward flexibility provision is convenient.

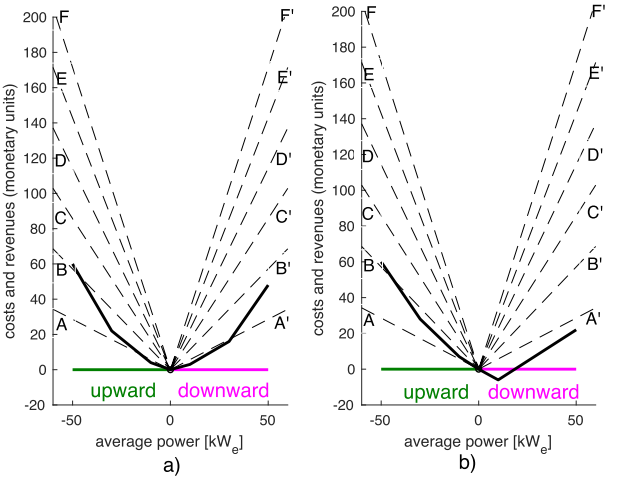

Fig. 24. ***Mapping of the extra costs (thick lines) and rewards (dashed lines) for changing the OP to provide flexibility services. (a) Initial optimal point. (b) Initial nonoptimal point.***

VII. CONCLUDING REMARKS

This article has shown that MES have an impressive potential to enhance flexibility with respect to what may be obtained in an electricity-only system. The connection of multiple MES within a DMES provides further opportunities to consider flexibility in a system-wide way. The DMES concept is scalable, considering different levels of MES aggregation (district-based, city-based, or regional) with the corresponding multienergy grid infrastructures that interconnect the individual systems. It has been shown that the presence of network constraints can affect the exploitable flexibility, because some energy flows become limited. Furthermore, the presence of intertemporal constraints, depending on ON/OFF switching and ramp-rates, introduces the notion of dynamic flexibility and further shrinks the size of the flexibility region around a given OP. Nevertheless, from the technical point of view, the exploitation of DMES to provide flexibility is a high-value asset.

From the practical point of view, all the components needed to implement the DMES concept do exist, and in particular, storage and conversion systems have been improved in recent years. Also from the modeling point of view, this article has highlighted the mathematical framework that can be used to evaluate the potential flexibility of DMES. In particular, the concept of multienergy node has been introduced by extending the general formulation of the power node used to assess the electrical flexibility to encompass the MES modeling framework typically described in the energy hub formulation. Furthermore, the representation of the flexibility can be effectively visualized through the application of feasibility and flexibility maps constructed by exploiting the Minkowski summation principle.

Further considerations concern the practical implementation of DMES to provide flexibility. The implementation of the DMES concept needs the presence of multienergy infrastructures already installed. In countries with limited infrastructure, the DMES concept can be applied to local energy systems, which are not interconnected to a national infrastructure. In this case, the exploitation of the renewable energy potential through DMES, together with the presence of electricity and heat (and in the case of hydrogen), can be the basis for a self-sustained energy system.

The proposed modeling framework based on multienergy node can be adopted to assess the development of more and increasingly important flexibility options and use cases relevant to DMES. For example, cities are the natural places where the DMES concept can be applied. However, in cities, different companies often operate different infrastructures, and the share of the infrastructure knowledge as well as their combined operation could be difficult. Even in the presence of the same multiutility, the combined and optimal operation of the system may result in a difficulty due to the absence of adequate mature tools for the combined planning and operation, whereas the existing methodologies are still at the research stage. In particular, if random variables are involved, or introduced, for example, by the uncertainty in energy demand or local generation (e.g., from RES) within the DMES, flexibility assessment needs to resort to a stochastic framework. In this respect, DMES stochastic flexibility is an important open research topic.

The exploitation of flexibility from DMES is also appropriate for the decarbonization of the energy sector. However, to make DMES more effective, there is a need for updated regulatory provisions that cover the DMES operation. While renewable energy is well defined on the electrical side, today, the lack of accurate definition of the meaning of renewable gas and renewable heat represents an obstacle to the real implementation of some energy conversion systems needed for DMES applications. Even after issuing proper definitions, the policies to promote the use of renewable gas and renewable heat would require at least an incentive scheme for covering the additional costs existing for their production.

Considering the abovementioned aspects and despite some existing limitations, DMES is a quite promising framework: the proper exploitation of its potential needs a strict collaboration between sectors, with strong interdisciplinary working groups properly addressing not only the typical problems of each domain but also the challenges coming from the interactions among the different domains. ■

APPENDIX
EFFICIENCY MATRICES FOR SOME MES COMPONENTS

For the CHP with electrical efficiency η_e^{CHP} and thermal efficiency η_h^{CHP}

$$\begin{bmatrix} 0 \\ P_o^{\mathrm{CHP}} \\ H_o^{\mathrm{CHP}} \end{bmatrix} = \begin{bmatrix} 0 & 0 & 0 \\ \eta_e^{\mathrm{CHP}} & 0 & 0 \\ \eta_h^{\mathrm{CHP}} & 0 & 0 \end{bmatrix} \begin{bmatrix} F_i^{\mathrm{CHP}} \\ 0 \\ 0 \end{bmatrix} \Leftrightarrow \mathbf{v}_o^{\mathrm{CHP}} = \mathbf{H}^{\mathrm{CHP}} \mathbf{v}_i^{\mathrm{CHP}}.$$

For the AB with thermal efficiency η_h^{AB}

$$\begin{bmatrix} 0 \\ 0 \\ H_o^{\mathrm{AB}} \end{bmatrix} = \begin{bmatrix} 0 & 0 & 0 \\ 0 & 0 & 0 \\ \eta_h^{\mathrm{AB}} & 0 & 0 \end{bmatrix} \begin{bmatrix} F_i^{\mathrm{AB}} \\ 0 \\ 0 \end{bmatrix} \Leftrightarrow \mathbf{v}_o^{\mathrm{AB}} = \mathbf{H}^{\mathrm{AB}} \mathbf{v}_i^{\mathrm{AB}}.$$

For the EHP operating in heat output mode, with Coefficient of Performance $\mathrm{COP}^{\mathrm{EHP}}$

$$\begin{bmatrix} 0 \\ 0 \\ H_o^{\mathrm{EHP}} \end{bmatrix} = \begin{bmatrix} 0 & 0 & 0 \\ 0 & 0 & 0 \\ 0 & \mathrm{COP}^{\mathrm{EHP}} & 0 \end{bmatrix} \begin{bmatrix} 0 \\ P_i^{\mathrm{EHP}} \\ 0 \end{bmatrix} \Leftrightarrow \mathbf{v}_o^{\mathrm{EHP}} = \mathbf{H}^{\mathrm{EHP}} \mathbf{v}_i^{\mathrm{EHP}}.$$

For the P2G with the efficiency η_f^{P2G} of the complete chain that includes the electrolyzer the methanation system

$$\begin{bmatrix} F_o^{\mathrm{P2G}} \\ 0 \\ 0 \end{bmatrix} = \begin{bmatrix} 0 & \eta_f^{\mathrm{P2G}} & 0 \\ 0 & 0 & 0 \\ 0 & 0 & 0 \end{bmatrix} \begin{bmatrix} 0 \\ P_i^{\mathrm{P2G}} \\ 0 \end{bmatrix} \Leftrightarrow \mathbf{v}_o^{\mathrm{P2G}} = \mathbf{H}^{\mathrm{P2G}} \mathbf{v}_i^{\mathrm{P2G}}.$$

REFERENCES

[1] H. Holttinen *et al.*, "The flexibility workout: Managing variable resources and assessing the need for power system modification," *IEEE Power Energy Mag.*, vol. 11, no. 6, pp. 53–62, Nov. 2013.

[2] B. Mohandes, M. S. E. Moursi, N. Hatziargyriou, and S. E. Khatib, "A review of power system flexibility with high penetration of renewables," *IEEE Trans. Power Syst.*, vol. 34, no. 4, pp. 3140–3155, Jul. 2019.

[3] J. Ma, V. Silva, R. Belhomme, D. S. Kirschen, and L. F. Ochoa, "Evaluating and planning flexibility in sustainable power systems," *IEEE Trans. Sustain. Energy*, vol. 4, no. 1, pp. 200–209, Jan. 2013.

[4] P. D. Lund, J. Lindgren, J. Mikkola, and J. Salpakari, "Review of energy system flexibility measures to enable high levels of variable renewable electricity," *Renew. Sustain. Energy Rev.*, vol. 45, pp. 785–807, May 2015.

[5] P. Mancarella, "MES (multi-energy systems): An overview of concepts and evaluation models," *Energy*, vol. 65, pp. 1–17, Feb. 2014.

[6] E. A. M. Cesena, N. Good, M. Panteli, J. Mutale, and P. Mancarella, "Flexibility in sustainable electricity systems: Multivector and multisector nexus perspectives," *IEEE Electrific. Mag.*, vol. 7, no. 2, pp. 12–21, Jun. 2019.

[7] E. Dall'Anese, P. Mancarella, and A. Monti, "Unlocking flexibility: Integrated optimization and control of multienergy systems," *IEEE Power Energy Mag.*, vol. 15, no. 1, pp. 43–52, Jan. 2017.

[8] L. Zhang, N. Good, and P. Mancarella, "Building-to-grid flexibility: Modelling and assessment metrics for residential demand response from heat pump aggregations," *Appl. Energy*, vols. 233–234, pp. 709–723, Jan. 2019.

[9] A. L. Landry, H. Wang, I. Shames, P. Mancarella, and J. Taylor, "Online convex optimization of multi-energy building-to-grid ancillary services," *IEEE Trans. Control Syst. Technol.*, to be published.

[10] N. Good and P. Mancarella, "Flexibility in multi-energy communities with electrical and thermal storage: A stochastic, robust approach for multi-service demand response," *IEEE Trans. Smart Grid*, vol. 10, no. 1, pp. 503–513, Jan. 2019.

[11] E. A. M. Cesena and P. Mancarella, "Energy systems integration in smart districts: Robust optimisation of multi-energy flows in integrated electricity, heat and gas networks," *IEEE Trans. Smart Grid*, vol. 10,

no. 1, pp. 1122–1131, Jan. 2019.
[12] P. Mancarella and G. Chicco, "Real-time demand response from energy shifting in distributed multi-generation," *IEEE Trans. Smart Grid*, vol. 4, no. 4, pp. 1928–1938, Dec. 2013.
[13] T. Capuder and P. Mancarella, "Techno-economic and environmental modelling and optimization of flexible distributed multi-generation options," *Energy*, vol. 71, pp. 516–533, Jul. 2014.
[14] P. Mancarella, G. Chicco, and T. Capuder, "Arbitrage opportunities for distributed multi-energy systems in providing power system ancillary services," *Energy*, vol. 161, pp. 381–395, Oct. 2018.
[15] J. Salpakari, J. Mikkola, and P. D. Lund, "Improved flexibility with large-scale variable renewable power in cities through optimal demand side management and power-to-heat conversion," *Energy Convers. Manage.*, vol. 126, pp. 649–661, Oct. 2016.
[16] S. Heinen, P. Mancarella, C. O'Dwyer, and M. O'Malley, "Heat electrification: The latest research in europe," *IEEE Power Energy Mag.*, vol. 16, no. 4, pp. 69–78, Jul. 2018.
[17] S. Clegg and P. Mancarella, "Integrated modeling and assessment of the operational impact of power-to-gas (P2G) on electrical and gas transmission networks," *IEEE Trans. Sustain. Energy*, vol. 6, no. 4, pp. 1234–1244, Oct. 2015.
[18] A. Mazza, E. Bompard, and G. Chicco, "Applications of power to gas technologies in emerging electrical systems," *Renew. Sustain. Energy Rev.*, vol. 92, pp. 794–806, Sep. 2018.
[19] A. Ulbig and G. Andersson, "Analyzing operational flexibility of electric power systems," *Int. J. Electr. Power Energy Syst.*, vol. 72, pp. 155–164, Nov. 2015.
[20] H. Wang, S. Riaz, and P. Mancarella, "Integrated techno-economic modeling, flexibility analysis, and business case assessment of an urban virtual power plant with multi-market co-optimization," *Appl. Energy*, vol. 259, Feb. 2020, Art. no. 114142.
[21] P. Mancarella and G. Chicco, "Integrated energy and ancillary services provision in multi-energy systems," in *Proc. IREP Symp. Bulk Power Syst. Dyn. Control IX Optim., Secur. Control Emerg. Power Grid*, Aug. 2013, pp. 1–19.
[22] Y. V. Makarov, C. Loutan, J. Ma, and P. de Mello, "Operational impacts of wind generation on california power systems," *IEEE Trans. Power Syst.*, vol. 24, no. 2, pp. 1039–1050, May 2009.
[23] H. Nosair and F. Bouffard, "Flexibility envelopes for power system operational planning," *IEEE Trans. Sustain. Energy*, vol. 6, no. 3, pp. 800–809, Jul. 2015.
[24] J. Hinker, H. Knappe, and J. M. A. Myrzik, "Precise assessment of technically feasible power vector interactions for arbitrary controllable multi-energy systems," *IEEE Trans. Smart Grid*, vol. 10, no. 1, pp. 1146–1155, Jan. 2019.
[25] S. Clegg and P. Mancarella, "Integrated electrical and gas network flexibility assessment in low-carbon multi-energy systems," *IEEE Trans. Sustain. Energy*, vol. 7, no. 2, pp. 718–731, Apr. 2016.
[26] M. Geidl, G. Koeppel, P. Favre-Perrod, B. Klockl, G. Andersson, and K. Fröhlich, "Energy hubs for the future," *IEEE Power Energy Mag.*, vol. 5, no. 1, pp. 24–30, Jan. 2007.
[27] M. Geidl, "Integrated modeling and optimization of multi-carrier energy systems," Ph.D. dissertation, ETH Zürich, 2007.
[28] K. Heussen, S. Koch, A. Ulbig, and G. Andersson, "Unified system-level modeling of intermittent renewable energy sources and energy storage for power system operation," *IEEE Syst. J.*, vol. 6, no. 1, pp. 140–151, Mar. 2012.
[29] J. H. Horlock, *Cogeneration-Combined Heat and Power (CHP)*. Malabar, FL, USA: Krieger, 1997.
[30] G. Chicco and P. Mancarella, "From cogeneration to trigeneration: Profitable alternatives in a competitive market," *IEEE Trans. Energy Convers.*, vol. 21, no. 1, pp. 265–272, Mar. 2006.
[31] L. D. D. Harvey, *A Handbook on Low-Energy Buildings and District-Energy Systems*. London, U.K.: Earthscan, 2006.
[32] K. Ghaib and F.-Z. Ben-Fares, "Power-to-methane: A state-of-the-art review," *Renew. Sustain. Energy Rev.*, vol. 81, pp. 433–446, Jan. 2018.
[33] M. Götz *et al.*, "Renewable power-to-gas: A technological and economic review," *Renew. Energy*, vol. 85, pp. 1371–1390, Jan. 2016.
[34] A. Valera-Medina, H. Xiao, M. Owen-Jones, W. I. F. David, and P. J. Bowen, "Ammonia for power," *Prog. Energy Combustion Sci.*, vol. 69, pp. 63–102, Nov. 2018.
[35] A. Yapicioglu and I. Dincer, "A review on clean ammonia as a potential fuel for power generators," *Renew. Sustain. Energy Rev.*, vol. 103, pp. 96–108, Apr. 2019.
[36] R. Andika *et al.*, "Co-electrolysis for power-to-methanol applications," *Renew. Sustain. Energy Rev.*, vol. 95, pp. 227–241, Nov. 2018.
[37] P. Mancarella and G. Chicco, *Distributed Multi-Generation Systems: Energy Models and Analyses*. New York, NY, USA: Nova Science Publisher, 2009.
[38] M. Geidl and G. Andersson, "Optimal power flow of multiple energy carriers," *IEEE Trans. Power Syst.*, vol. 22, no. 1, pp. 145–155, Feb. 2007.
[39] G. Chicco and P. Mancarella, "Matrix modelling of small-scale trigeneration systems and application to operational optimization," *Energy*, vol. 34, no. 3, pp. 261–273, Mar. 2009.
[40] Y. Wang, N. Zhang, C. Kang, D. S. Kirschen, J. Yang, and Q. Xia, "Standardized matrix modeling of multiple energy systems," *IEEE Trans. Smart Grid*, vol. 10, no. 1, pp. 257–270, Jan. 2019.
[41] A. Hajimiragha, C. Canizares, M. Fowler, M. Geidl, and G. Andersson, "Optimal energy flow of integrated energy systems with hydrogen economy considerations," in *Proc. iREP Symp. Bulk Power Syst. Dyn. Control VII Revitalizing Oper. Rel.*, Charleston, SC, USA, Aug. 2007, pp. 1–11.
[42] F. Kienzle, P. Ahcin, and G. Andersson, "Valuing investments in multi-energy conversion, storage, and demand-side management systems under uncertainty," *IEEE Trans. Sustain. Energy*, vol. 2, no. 2, pp. 194–202, Apr. 2011.
[43] N. Neyestani, M. Yazdani-Damavandi, M. Shafie-Khah, G. Chicco, and J. P. S. Catalao, "Stochastic modeling of multienergy carriers dependencies in smart local networks with distributed energy resources," *IEEE Trans. Smart Grid*, vol. 6, no. 4, pp. 1748–1762, Jul. 2015.
[44] J. M. Arroyo and A. J. Conejo, "Optimal response of a thermal unit to an electricity spot market," *IEEE Trans. Power Syst.*, vol. 15, no. 3, pp. 1098–1104, Aug. 2000.
[45] P. Mancarella and G. Chicco, "Operational optimization of multigeneration systems," in *Electric Power Systems Advanced Forecasting Techniques and Optimal Generation Scheduling*, J. P. S. Catalão, Ed. Boca Raton, FL, USA: CRC Press, 2012, ch. 10.
[46] Y. Wang, J. Cheng, N. Zhang, and C. Kang, "Automatic and linearized modeling of energy hub and its flexibility analysis," *Appl. Energy*, vol. 211, pp. 705–714, Feb. 2018.
[47] N. Good, L. Zhang, A. Navarro-Espinosa, and P. Mancarella, "High resolution modelling of multi-energy domestic demand profiles," *Appl. Energy*, vol. 137, pp. 193–210, Jan. 2015.
[48] P. Mancarella, "Cogeneration systems with electric heat pumps: Energy-shifting properties and equivalent plant modelling," *Energy Convers. Manage.*, vol. 50, no. 8, pp. 1991–1999, Aug. 2009.
[49] G. Buffo, P. Marocco, D. Ferrero, A. Lanzini, and M. Santarelli, "Power-to-X and power-to-power routes," in *Solar Hydrogen Production*, F. Calisi, M. Dentice, D'Accadia, M. Santarelli, A. Lanzini, and D. Ferrero, Eds. Amsterdam, The Netherlands: Elsevier, 2019, ch. 15.
[50] J. Silva *et al.*, "Estimating the active and reactive power flexibility area at the TSO-DSO interface," *IEEE Trans. Power Syst.*, vol. 33, no. 5, pp. 4741–4750, Sep. 2018.
[51] E. Dall'Anese, P. Mancarella, and A. Monti, "Unlocking flexibility: Integrated optimization and control of multienergy systems," *IEEE Power Energy Mag.*, vol. 15, no. 1, pp. 43–52, Jan. 2017.
[52] E. A. Martinez-Cesena *et al.*, "Integrated electricity-heat-gas systems: Techno-economic modelling, optimization and application to multi-energy districts," *Proc. IEEE*, to be published.
[53] A. Piacentino and F. Cardona, "An original multi-objective criterion for the design of small-scale polygeneration systems based on realistic operating conditions," *Appl. Thermal Eng.*, vol. 28, nos. 17–18, pp. 2391–2404, Dec. 2008.
[54] Y. Kitapbayev, J. Moriarty, and P. Mancarella, "Stochastic control and real options valuation of thermal storage-enabled demand response from flexible district energy systems," *Appl. Energy*, vol. 137, pp. 823–831, Jan. 2015.
[55] A. Navarro-Espinosa and P. Mancarella, "Probabilistic modeling and assessment of the impact of electric heat pumps on low voltage distribution networks," *Appl. Energy*, vol. 127, pp. 249–266, Aug. 2014.
[56] S. Clegg and P. Mancarella, "Integrated electricity-heat-gas modelling and assessment, with applications to the great Britain system. Part II: Transmission network analysis and low carbon technology and resilience case studies," *Energy*, vol. 184, pp. 191–203, Oct. 2019.
[57] J. C. Koj, C. Wulf, J. Linssen, A. Schreiber, and P. Zapp, "Utilisation of excess electricity in different power-to-transport chains and their environmental assessment," *Transp. Res. D, Transp. Environ.*, vol. 64, pp. 23–35, Oct. 2018.
[58] K. H. R. Rouwenhorst, A. G. J. Van der Ham, G. Mul, and S. R. A. Kersten, "Islanded ammonia power systems: Technology review & conceptual process T design," *Renew. Sustain. Energy Rev.*, vol. 114, Oct. 2019, Art. no. 109339.
[59] A. Bloess, W.-P. Schill, and A. Zerrahn, "Power-to-heat for renewable energy integration: A review of technologies, modeling approaches, and flexibility potentials," *Appl. Energy*, vol. 212, pp. 1611–1626, Feb. 2018.
[60] S. Clegg and P. Mancarella, "Storing renewables in the gas network: Modelling of power-to-gas (P2G) seasonal storage flexibility in low carbon power systems," *IET Gener., Transmiss. Distrib.*, vol. 10, no. 3, pp. 566–575, 2016.
[61] J. Speirs, P. Balcombe, E. Johnson, J. Martin, N. Brandon, and A. Hawkes, "A greener gas grid: What are the options," *Energy Policy*, vol. 118, pp. 291–297, Jul. 2018.
[62] X. Zhang, G. Strbac, F. Teng, and P. Djapic, "Economic assessment of alternative heat decarbonisation strategies through coordinated operation with electricity system–UK case study," *Appl. Energy*, vol. 222, pp. 79–91, Jul. 2018.
[63] G. Dispenza *et al.*, "Development of a solar powered hydrogen fueling station in smart cities applications," *Int. J. Hydrogen Energy*, vol. 42, no. 46, pp. 27884–27893, Nov. 2017.
[64] N. Good, E. Karangelos, A. Navarro-Espinosa, and P. Mancarella, "Optimization under uncertainty of thermal storage based flexible demand response with quantification of residential users' discomfort," *IEEE Trans. Smart Grid*, vol. 6, no. 5, pp. 2333–2342, 2015.
[65] S. Stinner, K. Huchtemann, and D. Müller, "Quantifying the operational flexibility of building energy systems with thermal energy storages," *Appl. Energy*, vol. 181, pp. 140–154, Nov. 2016.
[66] Z. Yifan *et al.*, "Power and energy flexibility of district heating system and its application in wide-area power and heat dispatch," *Energy*, vol. 190, Jan. 2020, Art. no. 116426.
[67] G. Reynders, R. A. Lopes, A. Marszal-Pomianowska, D. Aelenei, J. Martins, and D. Saelens, "Energy flexible buildings: An evaluation of definitions and quantification methodologies applied to thermal storage," *Energy Buildings*, vol. 166, pp. 372–390, May 2018.
[68] E. Guelpa and V. Verda, "Thermal energy storage in district heating and cooling systems: A review," *Appl. Energy*, vol. 252, Oct. 2019, Art. no. 113474.
[69] A. L. A. Syrri and P. Mancarella, "Reliability and risk assessment of post-contingency demand response in smart distribution networks," *Sustain. Energy,*

Grids Netw., vol. 7, pp. 1–12, Sep. 2016.
[70] G. Chicco and P. Mancarella, "Distributed multi-generation: A comprehensive view," *Renew. Sustain. Energy Rev.*, vol. 13, no. 3, pp. 535–551, Apr. 2009.
[71] X. Liu and P. Mancarella, "Modelling, assessment and sankey diagrams of integrated electricity-heat-gas networks in multi-vector district energy systems," *Appl. Energy*, vol. 167, pp. 336–352, Apr. 2016.
[72] C. Shao, X. Wang, M. Shahidehpour, X. Wang, and B. Wang, "An MILP-based optimal power flow in multicarrier energy systems," *IEEE Trans. Sustain. Energy*, vol. 8, no. 1, pp. 239–248, Jan. 2017.
[73] W. Huang, N. Zhang, Y. Wang, T. Capuder, I. Kuzle, and C. Kang, "Matrix modeling of energy hub with variable energy efficiencies," *Int. J. Electr. Power Energy Syst.*, vol. 119, Jul. 2020, Art. no. 105876.
[74] A. Vandermeulen, B. van der Heijde, and L. Helsen, "Controlling district heating and cooling networks to unlock flexibility: A review," *Energy*, vol. 151, pp. 103–115, May 2018.
[75] A. Antenucci and G. Sansavini, "Gas-constrained secure reserve allocation with large renewable penetration," *IEEE Trans. Sustain. Energy*, vol. 9, no. 2, pp. 685–694, Apr. 2018.
[76] E. S. Menon, *Gas Pipeline Hydraulics*. Boca Raton, FL, USA: CRC Press, 2005.
[77] V. Verda, M. Capone, and E. Guelpa, "Optimal operation of district heating networks through demand response," *Int. J. Thermodyn.*, vol. 22, no. 1, pp. 35–43, 2019.

ABOUT THE AUTHORS

Gianfranco Chicco (Fellow, IEEE) received the Ph.D. degree in electrotechnics engineering from the Politecnico di Torino (POLITO), Turin, Italy, in 1992.

He is currently a Full Professor of electrical energy systems with POLITO. His research interests include power system and distribution system analysis and optimization, multienergy systems optimization and planning, energy efficiency and environmental impact assessment, integration of distributed energy resources in the electrical networks, electrical load management, data analytics, and artificial intelligence applications to power and energy systems.

Dr. Chicco is a member of the Italian Association of Automation, Energy, Information and Telecommunications (AEIT). He received the title of Doctor Honoris Causa from the Politehnica University of Bucharest and the "Gheorghe Asachi" of Iasi, Romania, in 2017 and 2018, respectively. He is the Scientific Coordinator of the Torino unit of the Italian Consortium ENSIEL. He was the Conference Chair of the World Energy System Conference (WESC) 2006 and the IEEE Innovative Smart Grid Technologies (ISGT) Europe 2017. He is the Editor-in-Chief of *Sustainable Energy Grids and Networks*, Subject Editor of *Energy*, and Editor of the IEEE TRANSACTIONS ON SMART GRID, the IEEE TRANSACTIONS ON SUSTAINABLE ENERGY, and *Energies*.

Shariq Riaz (Member, IEEE) received the B.Sc. (Honors) and M.Sc. degrees in electrical engineering from the University of Engineering and Technology at Lahore, Lahore, Pakistan, in 2009 and 2012, respectively, and the Ph.D. degree from The University of Sydney, Sydney, NSW, Australia, in 2018.

He is currently working as a Research Fellow with the Power and Energy Systems Group, The University of Melbourne, Melbourne, VIC, Australia. His research interests include power system flexibility modeling, multienergy systems, and grid/market integration of renewable generation, storage, distributed energy resources, and prosumers.

Andrea Mazza (Member, IEEE) received the M.Sc. (Honors) and the Ph.D. degrees in electrical engineering from the Politecnico di Torino (POLITO), Turin, Italy, in 2011 and 2015, respectively.

He is currently an Assistant Professor with POLITO and his research activities include distribution system optimization, distribution system reliability, decision-making methods applied to the electricity system, integration of distributed energy resources and large power-to-methane plants in the electricity grid, and optimal integration of multivector distribution systems (heat, gas, and electricity).

Pierluigi Mancarella (Senior Member, IEEE) received the M.Sc. and Ph.D. degrees in electrical energy systems from the Politecnico di Torino, Turin, Italy, in 2002 and 2006, respectively.

He is currently the Chair Professor of electrical power systems with The University of Melbourne, Melbourne, VIC, Australia, and a Professor of smart energy systems with The University of Manchester, Manchester, U.K. His research interests include multienergy systems, grid integration of renewables, energy infrastructure planning under uncertainty, and reliability and resilience assessment of low-carbon networks.

Dr. Mancarella is an Editor of the IEEE TRANSACTIONS ON POWER SYSTEMS and the IEEE TRANSACTIONS ON SMART GRID, an Associate Editor of the IEEE SYSTEMS JOURNAL, and an IEEE Power and Energy Society Distinguished Lecturer.